ERDC/EL TR-08-39

US Army Corps
of Engineers®
Engineer Research and
Development Center

Environmental Quality and Installations Program

UXO Characterization: Comparing Cued Surveying to Standard Detection and Discrimination Approaches

Report 8 of 9
Marine Corps Base Camp Lejeune: UXO Characterization Using Magnetic and Electromagnetic Data

Stephen D. Billings, Leonard R. Pasion, Laurens Beran,
Kevin Kingdon, and Jon Jacobson

September 2008

Environmental Laboratory

Environmental Quality and Installations Program

ERDC/EL TR-08-39
September 2008

UXO Characterization: Comparing Cued Surveying to Standard Detection and Discrimination Approaches

Report 8 of 9
Marine Corps Base Camp Lejeune: UXO Characterization Using Magnetic and Electromagnetic Data

Stephen D. Billings, Leonard R. Pasion, Kevin Kingdon, and Jon Jacobson

Sky Research, Inc.
445 Dead Indian Memorial Rd.
Ashland, OR 97520-9706

Laurens Beran

Earth and Ocean Science Department
University of British Columbia
Vancouver, B.C., Canada, V6T 1Z4

Report 8 of 9

Prepared for Headquarters, U.S. Army Corps of Engineers
Washington, DC 20314-1000

Monitored by Environmental Laboratory
U.S. Army Engineer Research and Development Center
3909 Halls Ferry Road, Vicksburg, MS 39180-6199

Abstract: The collection, processing, interpretation, and analysis of electromagnetic (EM) and magnetometer data collected at Camp Lejeune are described. The discrimination challenge at the site was to identify larger ferrous UXO and the smaller 40-mm grenades while preventing excessive excavations of adapters. For EM-61 towed array data, the relative size of primary and secondary polarizations allowed many adapters to be rejected. The relative decay rate of the primary or secondary polarizations was effective in distinguishing many of the remaining adapters from the UXO. The standard deviation in a 0.5-m radius of the corresponding magnetic data was also highly discriminatory against the adapters. For the UXO/adapter discrimination problem, the EM-61/magnetometer combination had comparable performance to the EM-63 alone. When the 40-mm grenades were included as potential UXO, the EM-63 significantly outperformed the EM-61/magnetometer combination.

Contents

Figures and Tables

Figures

Tables

Preface

This report was prepared as part of the Congressional Interest Environmental Quality and Installations Program, Unexploded Ordnance (UXO) Focus Area, Contract No. W912HZ-04-C-0039, Purchase Request No. W81EWF-418-0425, titled, "UXO Characterization: Comparison of Cued-Surveying to Standard Detection and Standard Discrimination Approaches." Research was conducted by Sky Research, Inc., for the Environmental Laboratory (EL), U.S. Army Engineer Research and Development Center (ERDC), Vicksburg, MS. The following Sky Research personnel contributed to this report:

- Dr. Stephen D. Billings was the project Principal Investigator and oversaw the data collection and analysis of the field data, and produced the report for this segment of the project.
- Jon Jacobson processed the magnetometer and EM data sets and conducted the parametric inversions.
- Dr. Leonard R. Pasion conducted quality control of the parametric inversions.
- Kevin Kingdon assisted with the data collection and processing of the data.
- Joy Rogalla was the copy editor for this report.
- Messrs. Daniel Connoly, Jeff Reuter, Casey McDonald, and Craig Hyslop assisted with the EM-61, EM-63, and magnetometer data collection efforts.

The following UBC-GIF personnel contributed to this report:

- Laurens Beran assisted with the EM-63 data collection and provided advice and technical support for the statistical classifications and bootstrap analysis.

The following Tetra-Tech EMI personnel contributed to this report:

- Kevin Kobel was the UXO Technician responsible for safety and also collected the ground-truth information.

The work conducted at Camp Lejeune was supported by the U.S. Marine Corps, and in particular by Duane Richardson of the Range Control Office at the base.

This project was performed under the general supervision of Dr. M. John Cullinane, Jr., Technical Director, Military Environmental Engineering and Sciences, EL, and John H. Ballard, Office of Technical Director and UXO Focus Area Manager, EL. Reviews were provided by Ballard and Dr. Dwain Butler, Alion Science and Technology Corporation. Dr. Beth Fleming was Director, EL.

COL Gary E. Johnston was Commander and Executive Director of ERDC. Dr. James R. Houston was Director.

Acronyms

AHRS	Attitude-Heading Reference System
Am^2	Amperes meters squared (unit of dipole moment)
AUC	Area Under the Curve
BOR	Body of Revolution
Cm	centimeters
DoD	Department of Defense
DSB	Defense Science Board
EL	Environmental Laboratory
EM	Electromagnetic
EMI	Electromagnetic Induction
EOD	Explosives and Ordnance Division
ERDC	Engineer Research and Development Center
ESTCP	Environmental Security Technology Certification Program
FAR	False Alarm Rate
FPF	False Positive Fraction
GLRT	Generalized Likelihood Ratio Test
GPR	Ground Penetrating Radar
HEAT	High Explosive Anti-tank
IMU	Inertial Motion Unit
m	meter(s)
mm	millimeter(s)
nT	nanoTesla
OE	Ordnance and Explosive

PNN	Probabilistic Neural Network
P-O	Pasion-Oldenburg
ROC	Receiver Operating Characteristic
RTS	Robotic Total Station
SNR	Signal to Noise Ratio
TPF	True Positive Fraction
UBC	University of British Columbia
UBC-GIF	University of British Columbia – Geophysical Inversion Facility
UXO	Unexploded Ordnance

General Introduction

The clearance of military facilities in the United States contaminated with unexploded ordnance (UXO) is one of the most significant environmental concerns facing the Department of Defense. A 2003 report by the Defense Science Board (DSB) on the topic estimated costs of remediation in the tens of billions of dollars. The DSB recognized that development of effective discrimination strategies to distinguish UXO from non-hazardous material is one essential technology area where the greatest cost saving to the Department of Defense (DoD) can be achieved.

The objective of project W912HZ-04-C-0039, "UXO Characterization: Comparison of Cued-Surveying to Standard Detection and Standard Discrimination Approaches," was to research, develop, optimize, and evaluate the efficiencies of different modes of UXO characterization and remediation as a function of the density of UXO and associated clutter. Survey modes investigated in the research include:

1. Standard detection survey: All selected anomalies are excavated;
2. Advanced discrimination survey: Data collected in proximity to each identified anomaly are inverted for physics-based parameters and statistical or analytical classifiers are used to rank anomalies, from which a portion of the higher ranked anomalies are excavated;
3. Cued survey mode: Each selected anomaly is revisited with an interrogation platform, high-quality data are collected and analyzed, and a decision is made as to whether to excavate the item, or leave it in the ground.

Specific technical objectives of the research were to:

- Determine the feasibility and effectiveness of different interrogation approaches based on the cued-survey approach;
- Determine the feasibility and effectiveness of different interrogation sensors including magnetics, ground penetrating radar (GPR), and electromagnetic (EM) induction (EMI), and evaluate combinations of these sensors;
- Develop and evaluate the most promising interrogation platform designs;

- Develop optimal processing and inversion approaches for cued-interrogation platform data sets;
- Evaluate the data requirements to execute accurate target parameterization and assess the technical issues associated with meeting these requirements using detection and interrogation survey techniques;
- Determine which survey mode is most effective as a function of geological interference and UXO/clutter density;
- Investigate the feasibility and effectiveness of using detailed test-stand measurements on UXO and clutter to assist in the design of interrogation algorithms used in the cued-search mode.

The main areas of research involved in these coordinated activities include:

- Sensor phenomenology including GPR, EMI , and magnetometry;
- Data collection systems; platforms, field survey systems, field interrogation systems;
- Parameter estimation techniques; inversion techniques (single, cooperative, joint), forward-model parameterizations, processing strategies;
- Classification methods; thresholding, statistical models, information systems.

This report "UXO Characterization: Comparison of Cued Surveying to Standard Detection and Standard Discrimination Approaches: Report 8 of 9 – Marine Corps Base Camp Lejeune: UXO Characterization Using Magnetic and Electromagnetic Data" is one of a series of nine reports written as part of W912HZ-04-C-0039:

1. UXO Characterization: Comparing Cued Surveying to Standard Detection and Discrimination Approaches: Report 1 of 9 – Summary Report;
2. UXO Characterization: Comparing Cued Surveying to Standard Detection and Discrimination Approaches: Report 2 of 9 – Ground Penetrating Radar for Unexploded Ordnance Characterization; Fundamentals;
3. UXO Characterization: Comparing Cued Surveying to Standard Detection and Discrimination Approaches: Report 3 of 9 – Test Stand Magnetic and Electromagnetic Measurements of Unexploded Ordnance;
4. UXO Characterization: Comparing Cued Surveying to Standard Detection and Discrimination Approaches: Report 4 of 9 – UXO Characterization Using Magnetic, Electromagnetic, and Ground Penetrating Radar Measurements at the Sky Research Test Plot;

5. UXO Characterization: Comparing Cued Surveying to Standard Detection and Discrimination Approaches: Report 5 of 9 – Optimized Data Collection Platforms and Deployment Modes for Unexploded Ordnance Characterization;
6. UXO Characterization: Comparing Cued Surveying to Standard Detection and Discrimination Approaches: Report 6 of 9 – Advanced Electromagnetic and Magnetic Methods for Discrimination of Unexploded Ordnance;
7. UXO Characterization: Comparing Cued Surveying to Standard Detection and Discrimination Approaches: Report 7 of 9 – Marine Corps Base Camp Lejeune: UXO Characterization Using Ground Penetrating Radar;
8. UXO Characterization: Comparing Cued Surveying to Standard Detection and Discrimination Approaches: Report 8 of 9 – Marine Corps Base Camp Lejeune: UXO Characterization Using Magnetic and Electromagnetic Data;
9. UXO Characterization: Comparing Cued Surveying to Standard Detection and Discrimination Approaches: Report 9 of 9 – Former Lowry Bombing and Gunnery Range: Comparison of UXO Characterization Performance Using Area and Cued-interrogation Survey Modes.

1 Introduction

Marine Corps Base Camp Lejeune in North Carolina was investigated and subsequently chosen as a site for demonstration and validation of UXO remediation technologies. The primary motivation for choosing Camp Lejeune was its suitability for ground penetrating radar (GPR) surveying. GPR signals are absorbed at different rates depending on the local survey environment, which results in finite, site-specific, penetration depths. In general, sandy soils exhibit superior GPR performance over silty soils with significant clay content. It was anticipated that the soils at Camp Lejeune would provide an environment favorable for GPR surveying. As part of the GPR survey campaign, a significant amount of detection mode electromagnetic induction (EMI; Geonics EM-61 and Geonics EM-63) and magnetometry data were collected. This report describes the collection, processing, interpretation, and analysis of the EMI and magnetometer datasets. The GPR data and more details on the Camp Lejeune test site are provided in Report 7 of this series.

2 Discrimination Mode Surveys Conducted at Camp Lejeune

2.1. Test site history/characteristics

The characteristics of the test site are described in Report 7 of this series.

2.2. Pre-demonstration testing and analysis

Pre-demonstration testing and analysis at the site are described in Report 7 of this series.

2.3. Discrimination mode surveys conducted at Camp Lejeune

Three different discrimination mode surveys were conducted at Camp Lejeune:

1. Geonics EM-61 MKII towed array with Leica Robotic Total Station (RTS) and Crossbow Attitude-Heading Reference System (AHRS)-400 inertial motion unit (IMU) for position and orientation (Figures 1a and 1d).
2. Geonics EM-63 cart with Leica RTS and Crossbow AHRS-400 IMU for position and orientation (Figure 1c).
3. Geometrics G823 cesium vapor, quad-sensor magnetometer array with Leica RTS for position (Figure 1b).

More details on these surveys can be found in Billings et al. (2007) and images of each system used to collect data for this study are shown in Figure 1. Table A1 summarizes the daily activities during the study.

The G6 site at Camp Lejeune consisted of 16 tiles (50-m by 50-m) as shown in Figure 2. Full coverage surveys of the G6 site were undertaken using both Sky Research, Inc.'s EM-61 towed array and man-portable magnetometer array. Some areas of the site were inaccessible due to large pools of standing water and a small creek that flowed across the site. Inspection of the EM-61 towed array data revealed that grids F1, F2, G1, and G2 were highly cluttered with multiple overlapping anomalies (Figure 2). Therefore, these southern grids were avoided with the Geonics EM-63 cart, which focused on the northern set of grids. Six of the grids were surveyed (A1, A2, D1, D2, E1, and E2) with the EM-63.

(a)

(b)

(c)

(d)

Figure 1. Discrimination mode platforms used to collect data at Camp Lejeune: (a) Geonics EM-61 MKII towed array; (b) quad-sensor magnetometer array; (c) Geonics EM-63; (d) Leica RTS.

Figures 3, 4, and 5 provide more detailed views of targets from Tiles D1, D2, E1, and E2. The crosses on each of the maps indicate the location of items that were excavated so that ground-truth data are available (referred to as "validated" targets). Seventeen UXO items were emplaced in Tiles A1 and A2, while thirteen UXO items were emplaced in Tile D2 prior to surveying with the EM-63 (see Appendix B). The locations of the emplaced items are shown as triangles in Figure 5. The UXO were emplaced in Tile D2 after the area had already been surveyed with the EM-61 and magnetometer; therefore the locations are not plotted on the plans shown in Figures 2 and 3.

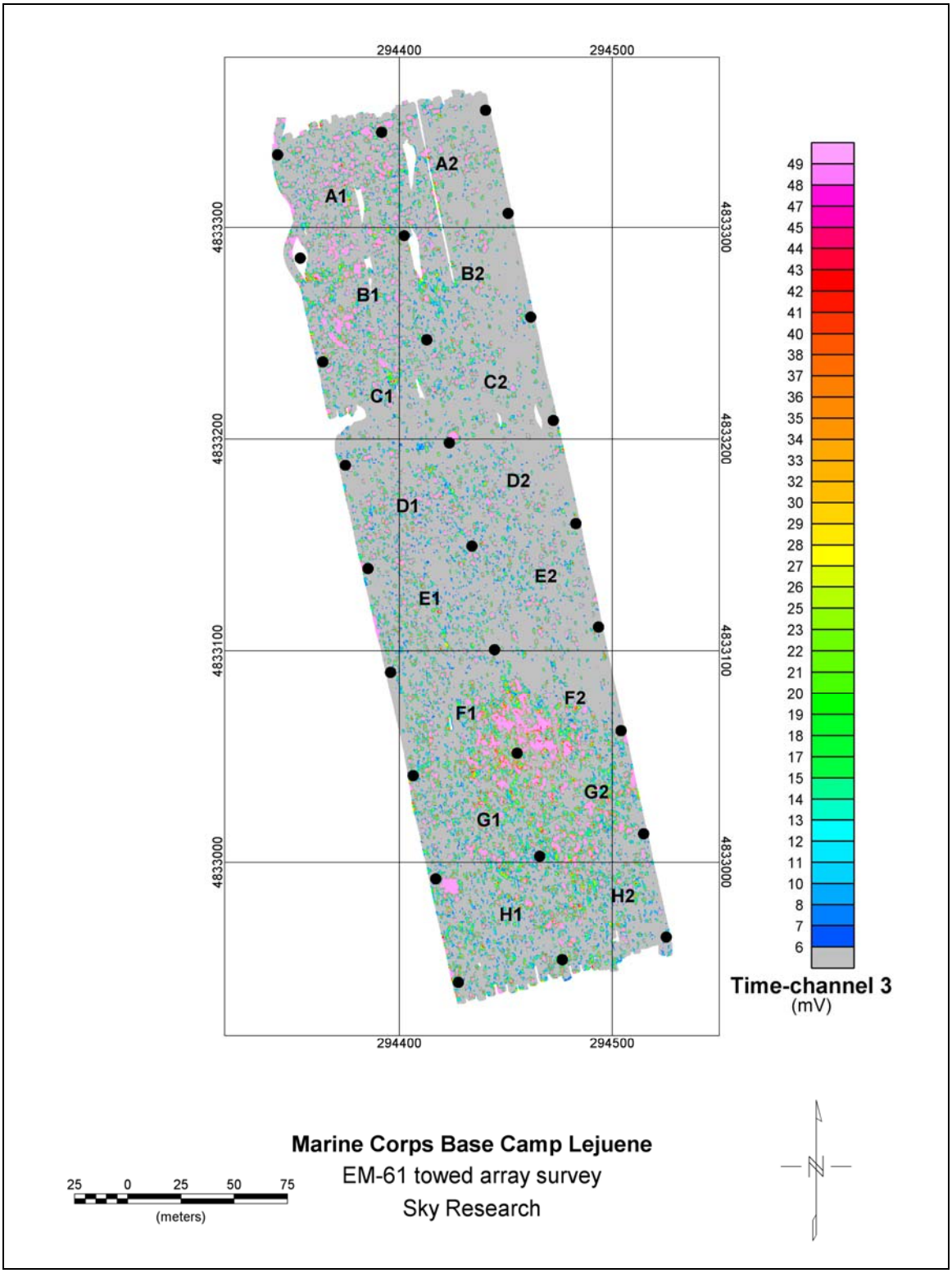

Figure 2. EM-61 towed array survey over the G6 Range at Camp Lejeune.

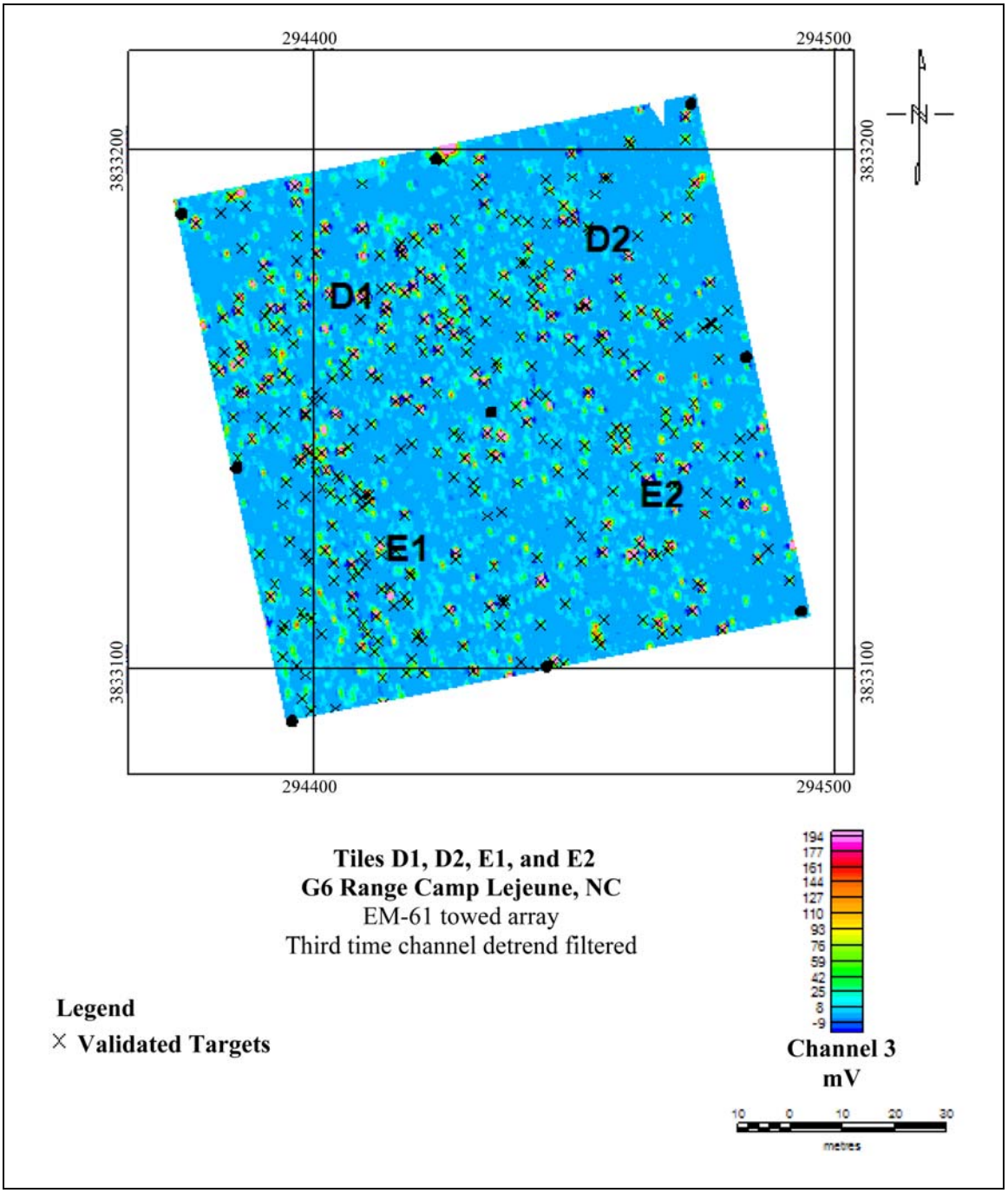

Figure 3. EM-61 towed array data from Tiles D1, D2, E1, and E2 on the G6 Range, Camp Lejeune, NC. The gridded image shown is the third time channel. The data have been detrend filtered. The black dots are the corners of the tiles. The crosses indicate the location of validated targets. There were no emplaced rounds on Tile D2 when this survey was conducted. The text indicates the tile names.

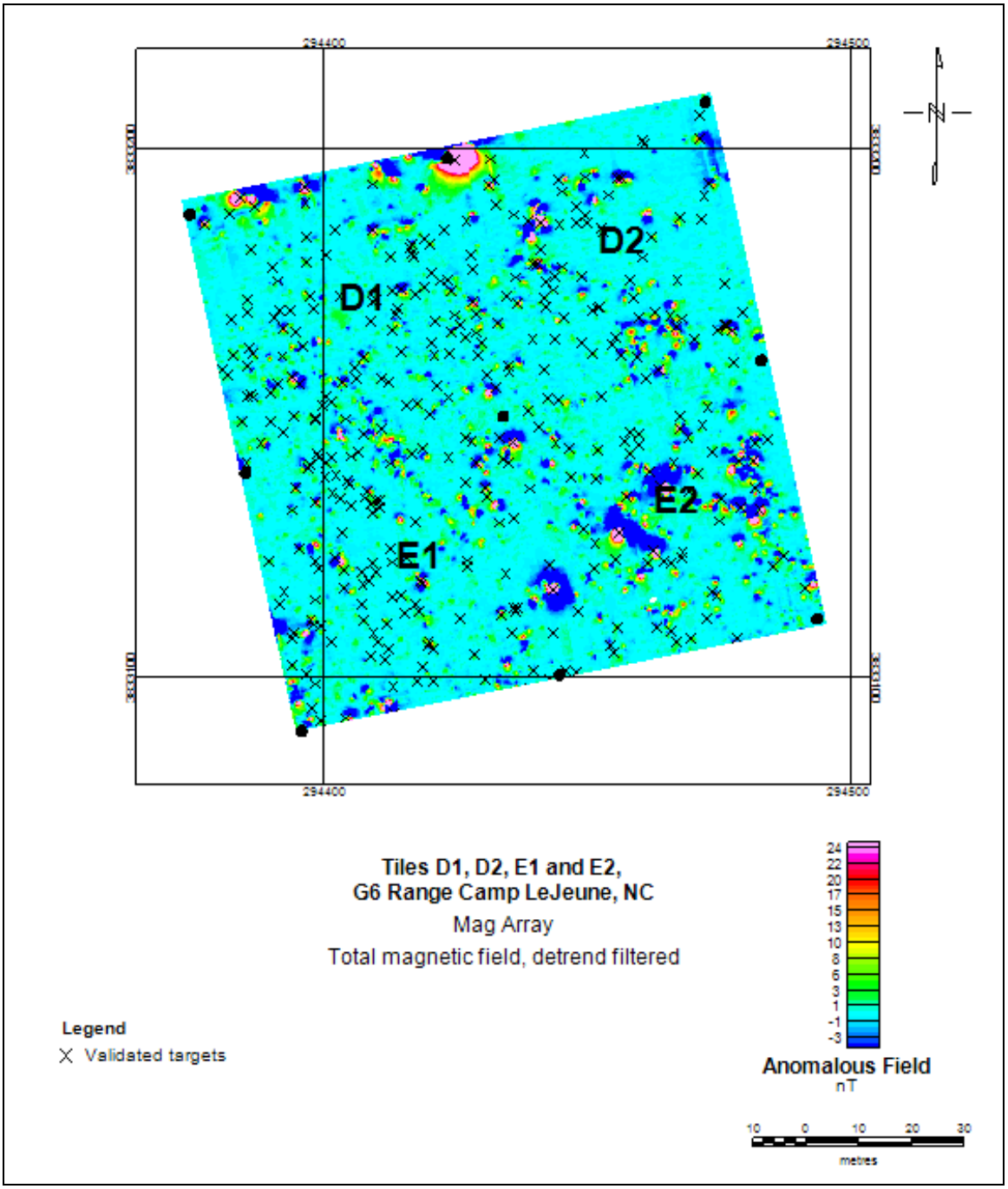

Figure 4. Magnetometer array data from Tiles D1, D2, E1, and E2 on the G6 Range, Camp Lejeune, NC. The gridded image shown is the total magnetic field. The data have been detrend filtered. The black dots are the corners of the tiles. The crosses indicate the location of validated targets. There were no emplaced rounds on Tile D2 when this survey was conducted. The text indicates the tile names.

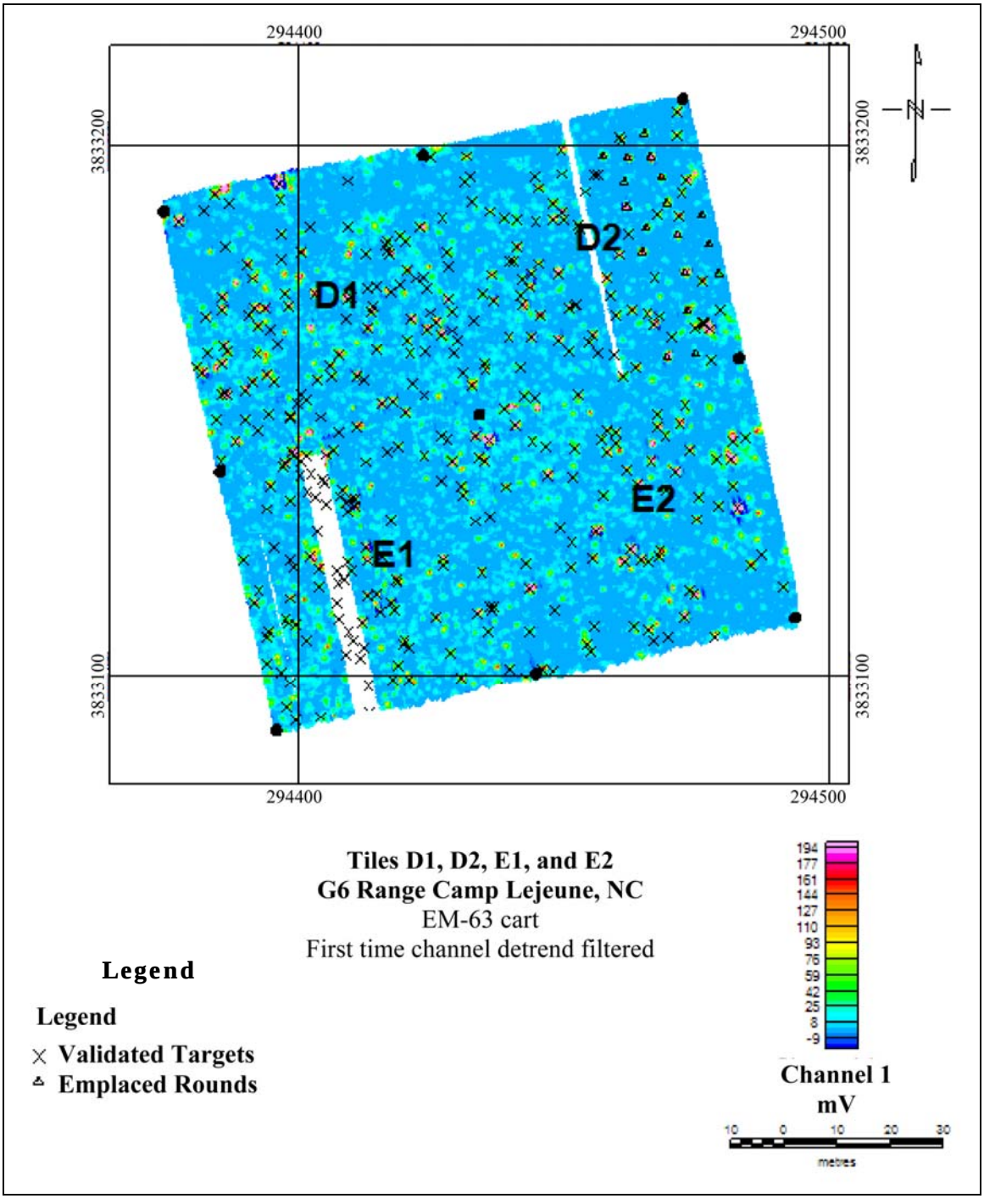

Figure 5. EM-63 cart data from Tiles D1, D2, E1, and E2 on the G6 Range, Camp Lejeune, NC. The gridded image shown is the first time channel. The data have been drift corrected and line leveled. The black dots are the corners of the tiles. The crosses indicate the location of validated targets and the triangles indicate the location of emplaced rounds.

2.4. Anomaly validation

Thirty inert ordnance items (all larger than 76 mm) were emplaced at the site (see Table B1). Ground-truth data were collected for 837 anomalies (Table 1) identified in the EM-61 or magnetometer datasets. Only one large UXO was encountered (a 120-millimeter (mm) HEAT [high explosive anti-tank] rocket) and this was left in place for follow-up by Marine Corps explosive ordnance division (EOD) personnel. They moved the item and then discovered that it was a high-explosive live round, at which point they destroyed it. One-hundred and seventeen 40-mm practice or smoke grenades recovered at the site were considered to be UXO. Adapters from discarding sabot munitions were the most ubiquitous ordnance and explosive (OE) scrap item and comprised over one-third of the recovered ground-truth items. The rest of the items were OE scrap, shrapnel, small arms munitions, or junk. Most of the excavations were conducted in the A, B, D, and E grids. As EM-63 data were not collected over the B grids, less ground-truth is available to assess the performance of that system.

Table 1. Summary of the ground-truth data collected on the G6 range at Camp Lejeune.

Anomaly	Number
Rocket 120 mm	1
40 mm	117
Adapter (or adapter part)	330
OE scrap	86
Small arms	46
Frag	89
Non OE related junk	168
Total	837

The objective of discrimination at the G6 range was to prevent excavation of large numbers of adapters, while ensuring that all 40-mm grenades and the one rocket were recovered.

2.5. Dipole model fitting

Each data set was preprocessed using the methods described in Report 6. A dipole model was then fit to each data set as follows:

1. For magnetics data, a static magnetic dipole was fit to the detrended total-magnetic field data.
2. For the EM-61 data, an instantaneous amplitude, two-polarization model was fit to all four time channels.
3. For the EM-63 data, two-polarization, Pasion-Oldenburg models (Pasion and Oldenburg 2001)

$$L_i(t) = k_i (t+\alpha_i)^{-\beta_i} \exp\left(-t / \gamma_i\right) \quad (1)$$

with $\alpha_i = 0$ and $i = \{1, 2, 3\}$, were fit to the 26 recorded time channels.

A visual review of the resulting fits determined if the model adequately represented the data. Example inversions from each data set are presented in Figures 6 through 9.

Figure 6. Examples of ground-truth data collected on Range G6, including a 120-mm HEAT Rocket (top left), 40-mm practice grenade (top right), adapter (center left), adapter part (center right), part of a discarding sabot and other OE scrap (bottom left), and four steel pipes (bottom right).

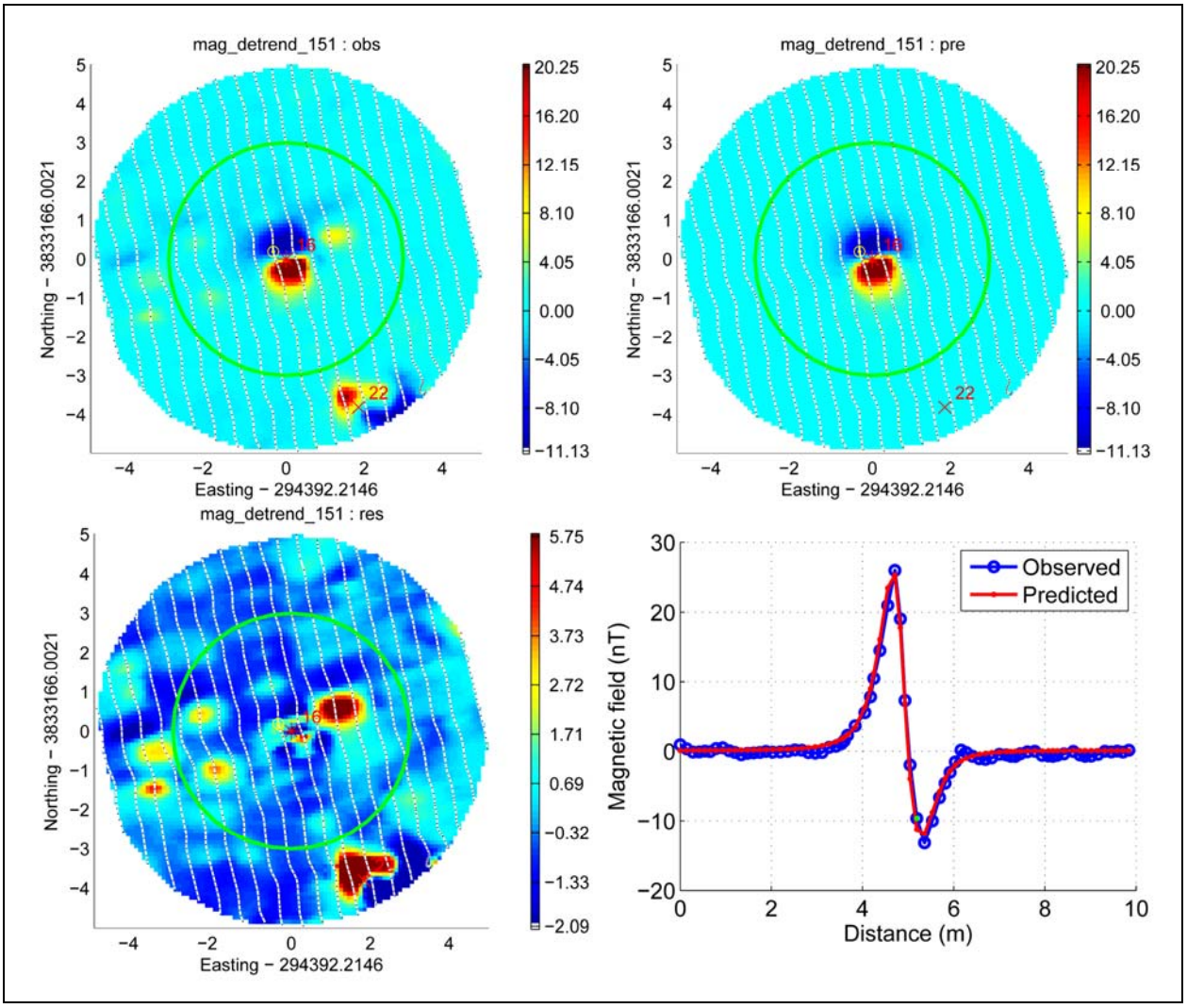

Figure 7. Example dipole model fit to a magnetic anomaly on grid D1. Observed data (upper right); predicted from best-fit model (upper left); residual (observed minus predicted; lower right); and observed versus predicted N-S profile (lower right). Notice the small overlapping anomaly to the northeast of the main anomaly. It is more evident in the residual plot, which has a different color scale.

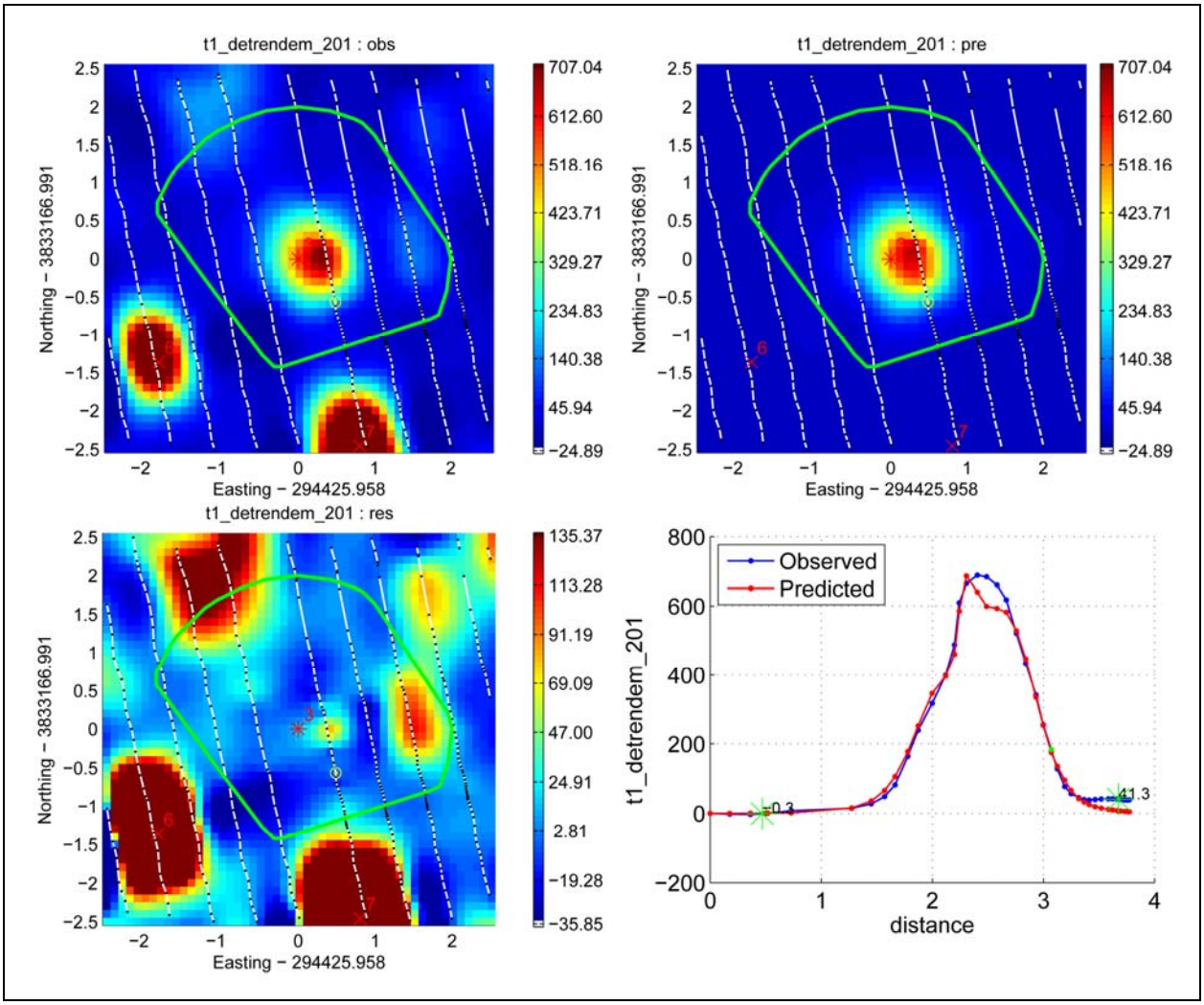

Figure 8. Example instantaneous amplitude model fit to time channel 1 of the EM-61 data collected over an adaptor on grid D1. Observed data (upper right); predicted from best-fit model (upper left); residual (observed minus predicted; lower right); and observed versus predicted N-S profile (lower right). Note color-scale difference for the residual plot.

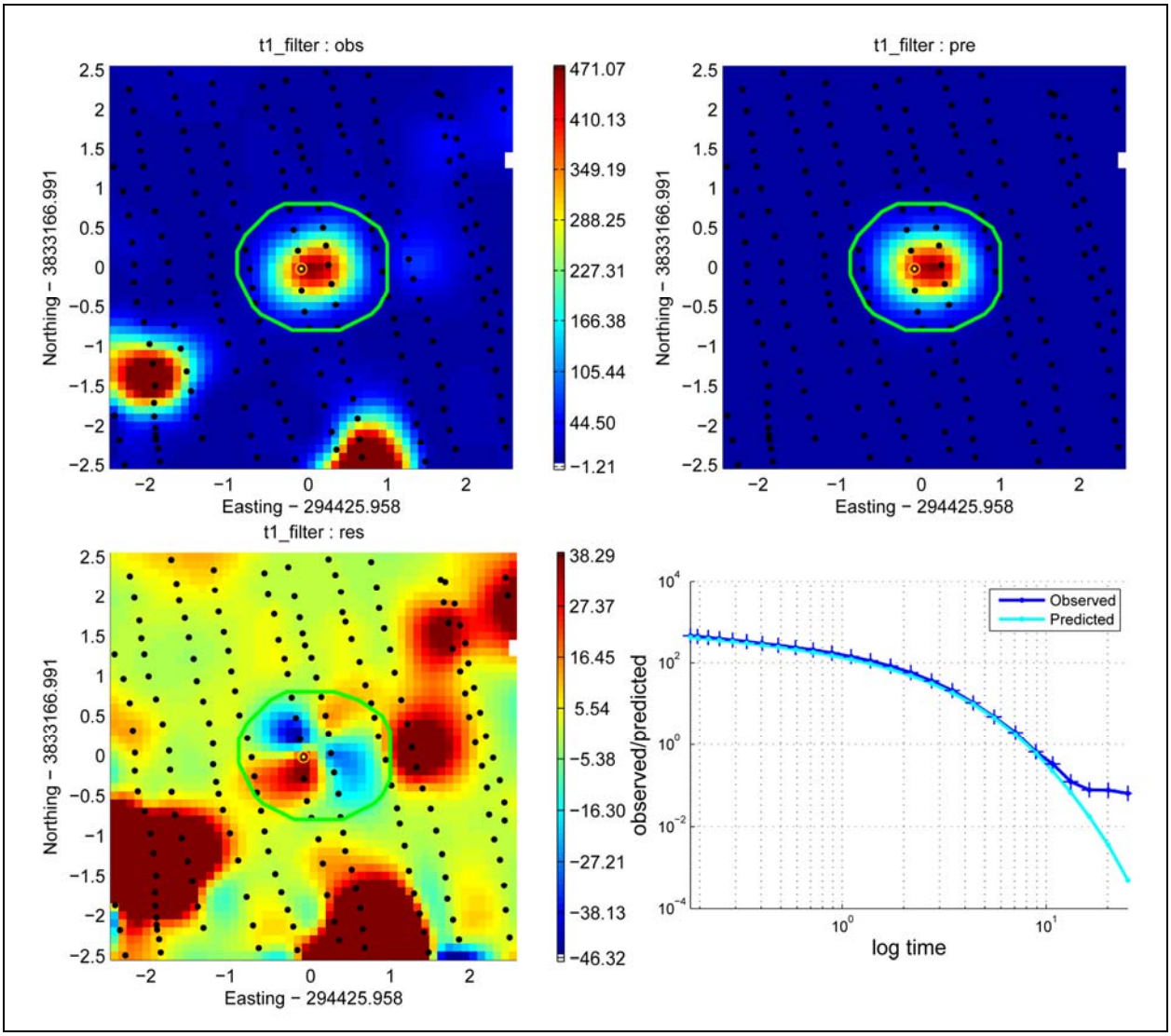

Figure 9. Example EM-63 Pasion-Oldenburg model fit to an adaptor on grid D1. Observed time channel 1 data (upper right); time channel 1 predicted from best-fit model (upper left); time channel 1 residual (observed minus predicted; lower right); and observed versus predicted sounding for the point with maximum amplitude (lower right). Note color-scale difference for the residual plot. Time channel 1 is 180 µs after pulse turn-off.

3 Comparison of Discrimination Performance

The discrimination challenge at Camp Lejeune was as follows:

1. Find all ferrous UXO items with caliber of 76 mm or greater;
2. Avoid digging the non-ferrous adapters and other non-hazardous items;
3. Find all 40-mm grenades (they are all non-ferrous).

Note that the last discrimination objective is likely to be difficult and of unknown priority (given this was an active range). Most of the 40-mm grenades were inert practice rounds, but some were smoke grenades that are potentially hazardous. Items 1 and 2 are considered the primary objectives; the change in discrimination performance will be evaluated when the third objective is included.

3.1. Magnetometer data

The magnetometer data included 168 anomalies with corresponding ground truth (including 16 emplaced items). Ten of the anomalies could not be reliably inverted for a dipole model (typically because of overlap with an adjacent item). The magnetometer data respond only to ferrous targets, which immediately provides a mechanism to avoid the non-ferrous adapters but also precludes discrimination success for the 40-mm grenades (which are typically aluminum). Figures 10a and 10b show the recovered moments of the various categories of items along with the *dipole feasibility curves* for 76-, 81-, 90-, 105-, and 155-mm caliber ordnance. The dipole feasibility curves trace all the dipole moments that could arise from induced magnetization alone and were obtained using the equivalent spheroid dimensions reported in Billings et al. (2006). Most of the emplaced ordnance items lie relatively close to one or more of the dipole feasibility curves, with two exceptions. These are the items with moments greater than four amperes meters squared (Am^2), which are visible in Figure 10a. These emplaced rounds have large remanent magnetizations, as they were not shock-demagnetized, which would (presumably) be the case for unexploded projectiles.

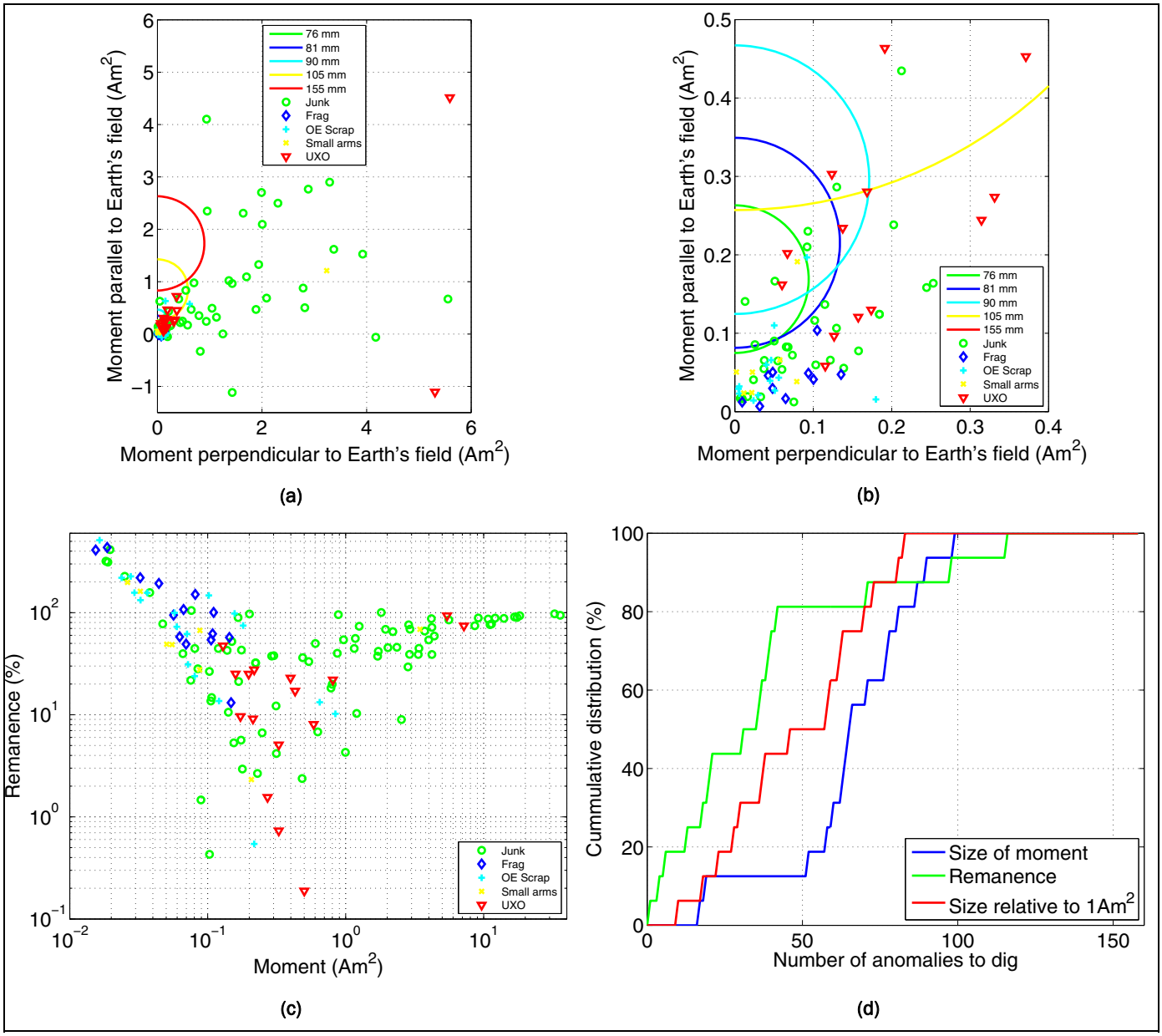

Figure 10. Feature vectors extracted from the magnetometer-array data including moments parallel (a) and perpendicular (b) to the Earth's field; and (c) moment versus remanence. In (d) an ROC curve for dig lists prioritized by remanence, size of moment, and size relative to 1 Am² are shown.

Billings (2004) has suggested that the *remanent magnetization metric* (otherwise known as the remanence metric) is an efficient method to prioritize a dig-list. To calculate the remanence metric, first find the point on the dipole feasibility curve that is closest to the fitted moment in question. Then calculate the "distance" d between the dipole and the point on the curve and finally calculate the remanence as r = 100 * d/m, where m is the magnitude of the dipole. For points on the curve, d = 0 and consequently r = 0. As the distance between the dipole and the curve increases,

so will the remanence. Figure 10c shows the amplitude of the moment and the estimated *remanent magnetization* of each item. Figure 10c plots the magnitude of the moment and the estimated remanence; it is evident that most of the UXO have low remanence. Figure 10d plots Receiver Operating Characteristic (ROC) curves for dig-lists based on remanence and on the size of the dipole moment. Remanence is initially the most efficient method with 13 of 16 UXOs recovered after digging 40 holes. However, due to the high remanent magnetization in some of the emplaced rounds, the final three items require much more digging to recover. With the potential for high remanence items, a method based on moment magnitude may be preferable. Digging in the order of largest to smallest moment does not result in a very efficient digging order because many of the larger fitted moments are due to large pieces of junk. Figure 10c shows that many of the UXO have moments between 0.1 and 7 Am^2. A simple way to bias the digging order to items of this size is to transform the moment using $|\log_{10}(m)|$ and then rank from smallest to largest. This method requires the least amount of digging to recover all 16 UXO, although it is not as effective as remanence in the initial stages of digging.

3.2. EM-61 towed array

There were 378 EM-61 anomalies that had valid three-dipole model fits with corresponding ground truth. A significant number (over 100) of anomalies over large surface or near-surface pieces of junk could not be fit with a polarization tensor model. Particularly prevalent were fence posts, long lengths of wire, and large pieces of targets that had fragmented during live firing.

The size and relative values of the three polarizations potentially provide information about the size, shape, and material composition of buried targets. For instance, a ferrous body-of-revolution (BOR) (like most UXO) has one large axial polarization and two smaller transverse polarizations. In contrast, an aluminum BOR has one small axial polarization and two larger transverse polarizations. Lastly, an irregular piece of shrapnel or junk will typically have three distinct polarizations.

The three polarizations are ordered using the values at the first time channel such that $L_1(t_1)$ has the largest value, followed by $L_2(t_1)$, and then $L_3(t_1)$. The spread in secondary and tertiary polarizations is defined as $[L_2(t_1) - L_3(t_1)]/L_2(t_1)$, and the ratio of primary to secondary polarizations as $L_2(t_1)/L_1(t_1)$. The spread would be zero for a ferrous BOR and non-zero

for an asymmetric object, while the ratio would be one for an aluminum BOR. Figure 11a plots these two quantities where it is apparent that there are no consistent patterns within each anomaly class. Thus, it is clear that the signal-to-noise ratio SNR, positional precision, and data density are insufficient to use the relative polarizations to determine if an object is a BOR.

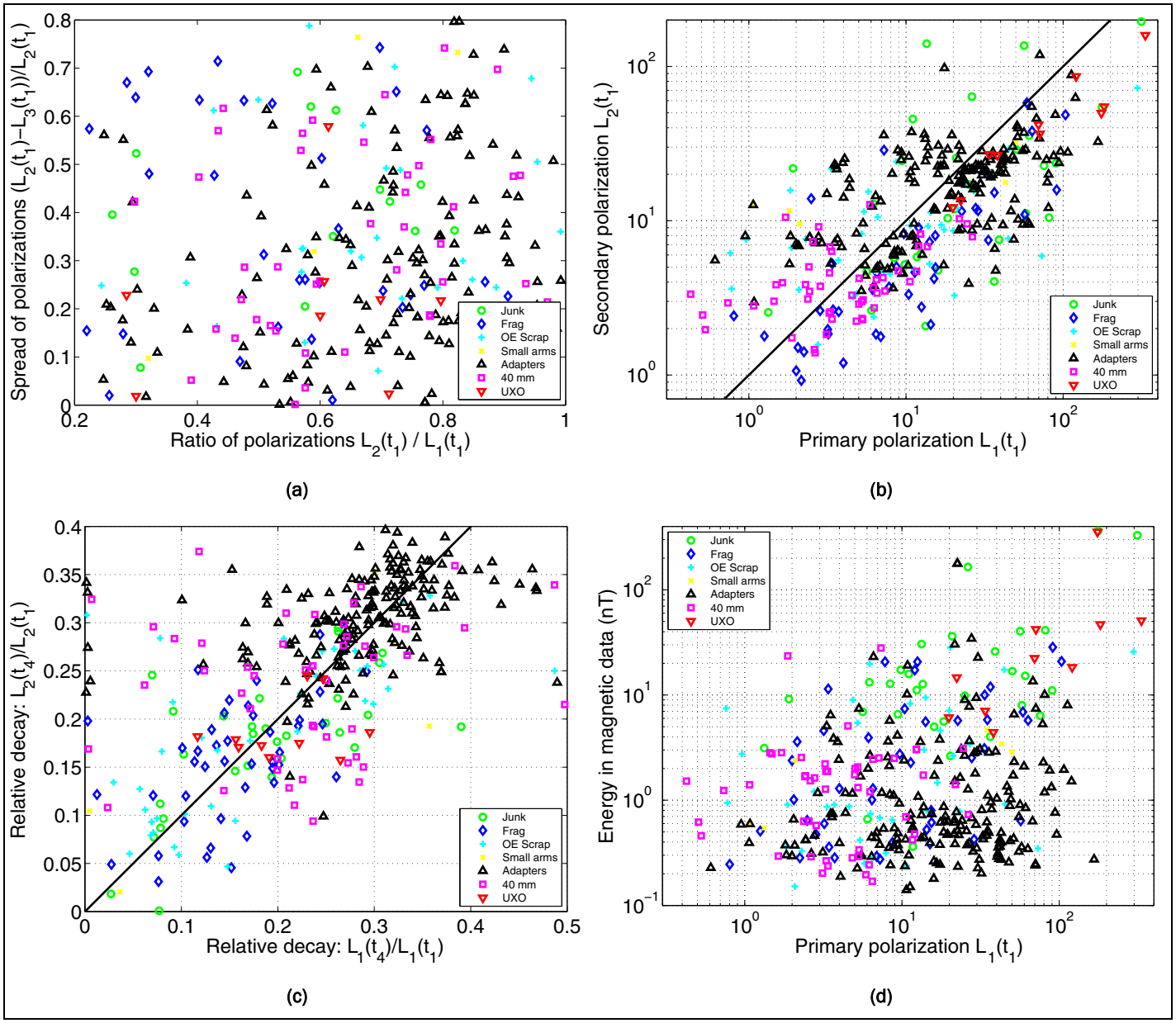

Figure 11. Feature vectors extracted from EM-61 towed array including (a) spread of secondary and tertiary polarizations versus ratio of primary to secondary polarization; (b) instantaneous primary and secondary polarizations at time channel 1; (c) relative decay rates of primary and secondary polarizations; and (d) primary polarization versus the energy in a 0.5-m radius circle in the magnetic data.

A more successful discrimination diagnostic can be obtained by comparing $L_1(t_1)$ - $L_2(t_1)$ to $L_2(t_1)$ - $L_3(t_1)$. If the former is larger, it can be assumed that a potential ferrous BOR exists and then $L'_1(t_1) = L_1(t_1)$ and $L'_2(t_1) = L'_3(t_1) = L_2(t_1)$. Otherwise, assume a potential non-ferrous BOR and set $L'_1(t_1) = L_3(t_1)$ and $L'_2(t_1) = L'_3(t_1) = L_1(t_1)$. This procedure effectively converts the three-dipole model into a two-dipole model and results in the feature space shown in Figure 11b. Anything above the 1:1 line is more likely aluminum and thus not a ferrous BOR. It is evident that many, but not all, of the adapters and 40-mm grenades lie above the line, while all the UXO fall below the line. In addition, the 40-mm grenades have small $L'_1(t_1)$, while the UXO and most adapters have larger $L'_1(t_1)$. A potential discrimination strategy is to dig all the small items (to recover the 40-mm grenades) and all large items with $L'_1(t_1) > L'_2(t_1)$. This would still result in the excavation of large numbers of adapters.

As a final means of reducing the number of adapters to dig (without resorting to the magnetic data), the relative decay of the L'_1 and L'_2 defined as $L'_1(t_4)/ L'_1(t_1)$ and $L'_2(t_4)/ L'_2(t_1)$, respectively, can be used. The adapters tend to have slower (and hence larger) relative decays and occupy a distinct region of feature space relative to the UXOs (Figure 11c). Thus, these features have good discrimination potential.

The final feature considered is the standard deviation of the magnetic data in a 0.5-m radius circle centered on the predicted dipole location. This measure is essentially equivalent to the energy in the magnetic data and will be small over adapters which are invisible to magnetometry (Figure 11d). The smallest value for a UXO is 4 nT, which is larger than the value over most adapters. Thus, including the magnetic data has the potential to significantly reduce the number of adapters excavated as suspected UXO.

3.3. EM-63 cart data

Using ground-truth and valid three-dipole model fits, 212 EM-63 anomalies occurred, including the fits over 21 emplaced UXO items of 76-mm caliber or larger. As per the EM-61 data, the spread and ratio of polarizations did not provide any diagnostic information and the three-dipole fits were converted to two-dipole fits using the same procedures (as the EM-61). In addition to the discrimination mode data, “test stand” quality data were also collected over the adapters in a test pit. This resulted in Pasion-Oldenburg parameters of $k_1 = 9.9170$, $k_2 = 11.1397$, $\beta_1 = 0.2887$,

β_2 = 0.2880, γ_1 = 1.8133, and γ_2 = 1.3157. These "test stand" parameters are shown in Figures 12a, 12c, and 12d as a magenta circle. Some variation is expected in the recovered parameters compared to these values as some adapters had end-caps, some did not, and some were just the end-caps themselves. Comparing k_1 and k_2 in Figure 12a, the same general comments apply as per the comparison of k_1 and k_2 from the EM-61 data. That is, many of the adapters lie above the 1:1 line (indicated as non-ferrous BOR) while all the UXO fall below this line. The 40-mm grenades are small and lie on both sides of the line. Including the standard deviation of the magnetic data would allow many of the adapters to be rejected (Figure 12b).

The Pasion-Oldenburg β and γ parameters control the time-decay behavior of the polarizations (Figures 12c and 12d). The values for the adapters are generally quite distinct from the UXO, particularly for the secondary polarization and would appear to provide a good mechanism for discrimination. This observation is reinforced by a plot of the normalized polarization tensors[1] of the primary and secondary polarizations of adapters, UXO, and 40-mm grenades (Figure 13). The recovered polarizations over the adapters are similar to the adapter test-stand polarization fit. The polarization decays of the UXO are different in character from the adapters, with a much faster decrease in amplitude at early times. In addition, many of the UXO have slower late-time decays compared to the rapid decrease in amplitude exhibited by the adapters.

3.4. Location and depth accuracy

Figures 14 and 15 compare the accuracy of the positions and depths predicted using the magnetometer, EM-61, and EM-63 data. Locations from the EM-63 data are more accurate than both the magnetometer and EM-61 predictions. The magnetic data are the least accurate, but that is potentially a sampling issue: many of the magnetometer anomalies were from large pieces of junk and it is difficult to accurately assign the position of an object with a large spatial extent. Depth predictions of the magnetometer and EM-63 data are comparable, with the EM-61 array slightly worse (Figure 15). Both of the EM models have a tendency to predict greater depths for the shallower items.

[1] Normalized as $L(t_n) / L(t_1)$.

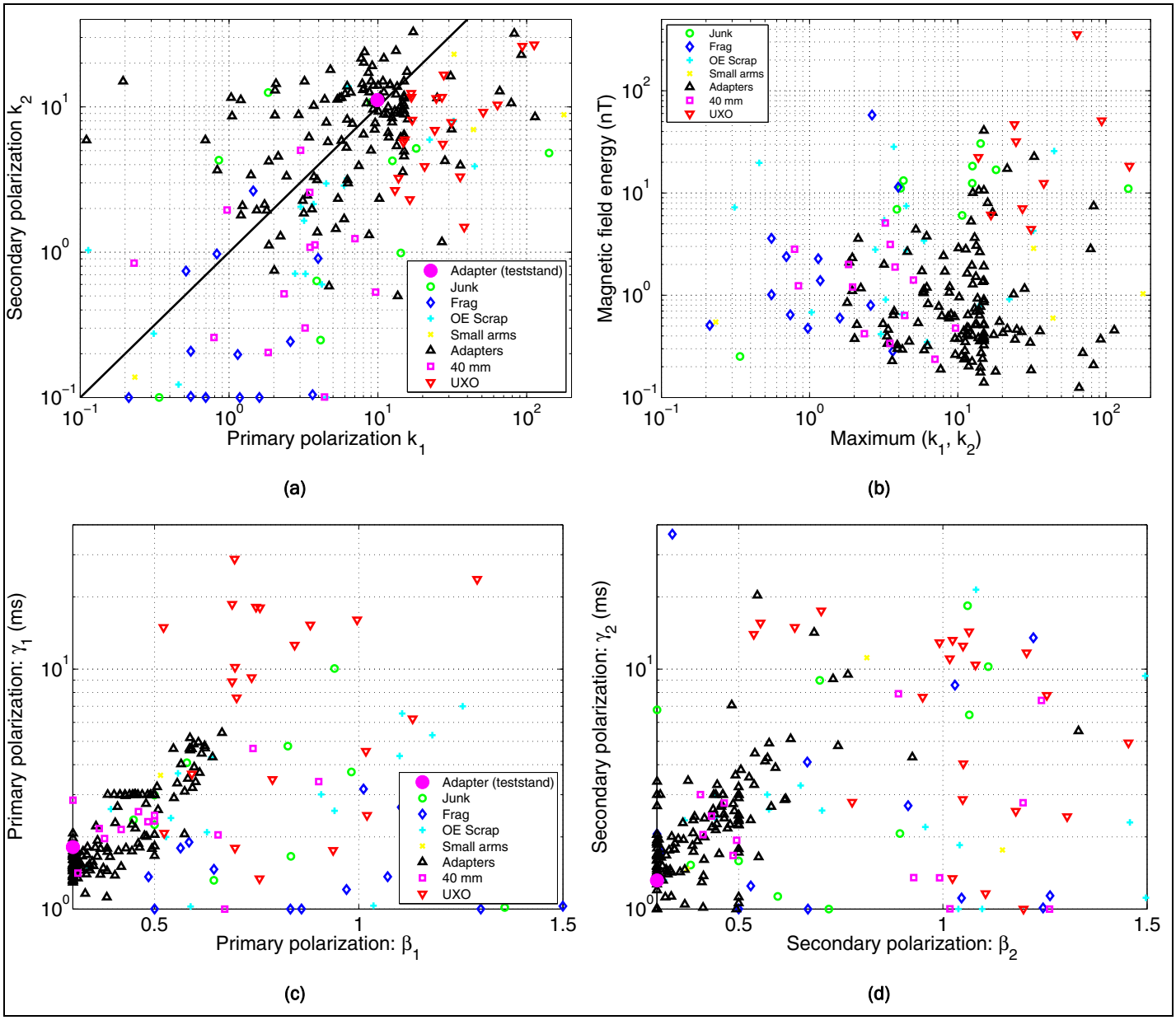

Figure 12. Feature vectors extracted from EM-63 cart data including (a) k_1 versus k_2; (b) maximum of k_1 and k_2 versus the energy in a 0.5-m radius circle in the magnetic data; (c) β and γ parameters from the primary polarization; and (d) β and γ parameters from the secondary polarization. In (a), (c), and (d), the feature vector extracted from "test-stand" quality EM-63 data is plotted.

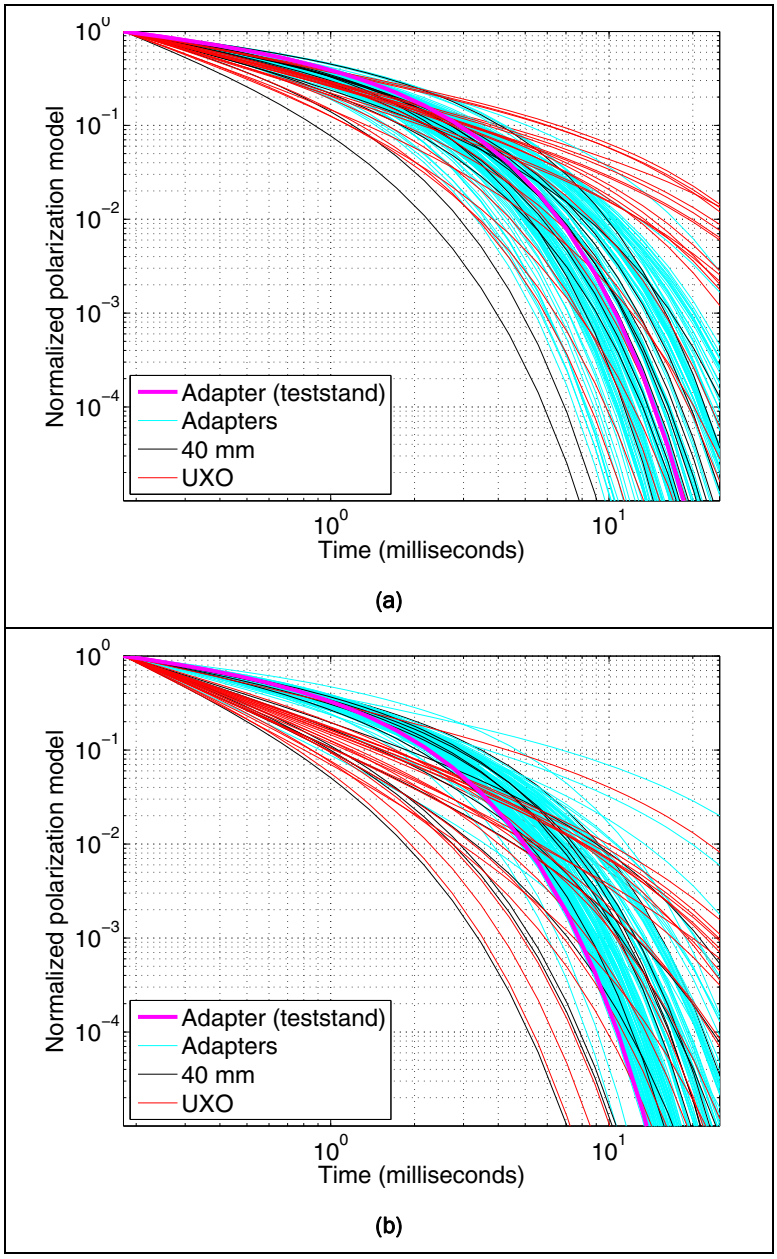

Figure 13. Primary (a) and secondary (b) polarizations recovered from EM-63 cart data over UXO, adapters, and 40-mm grenades. The polarization curves were obtained from the best-fit Pasion-Oldenburg parameters to each anomaly, and have been normalized to have unit polarization at time channel 1.

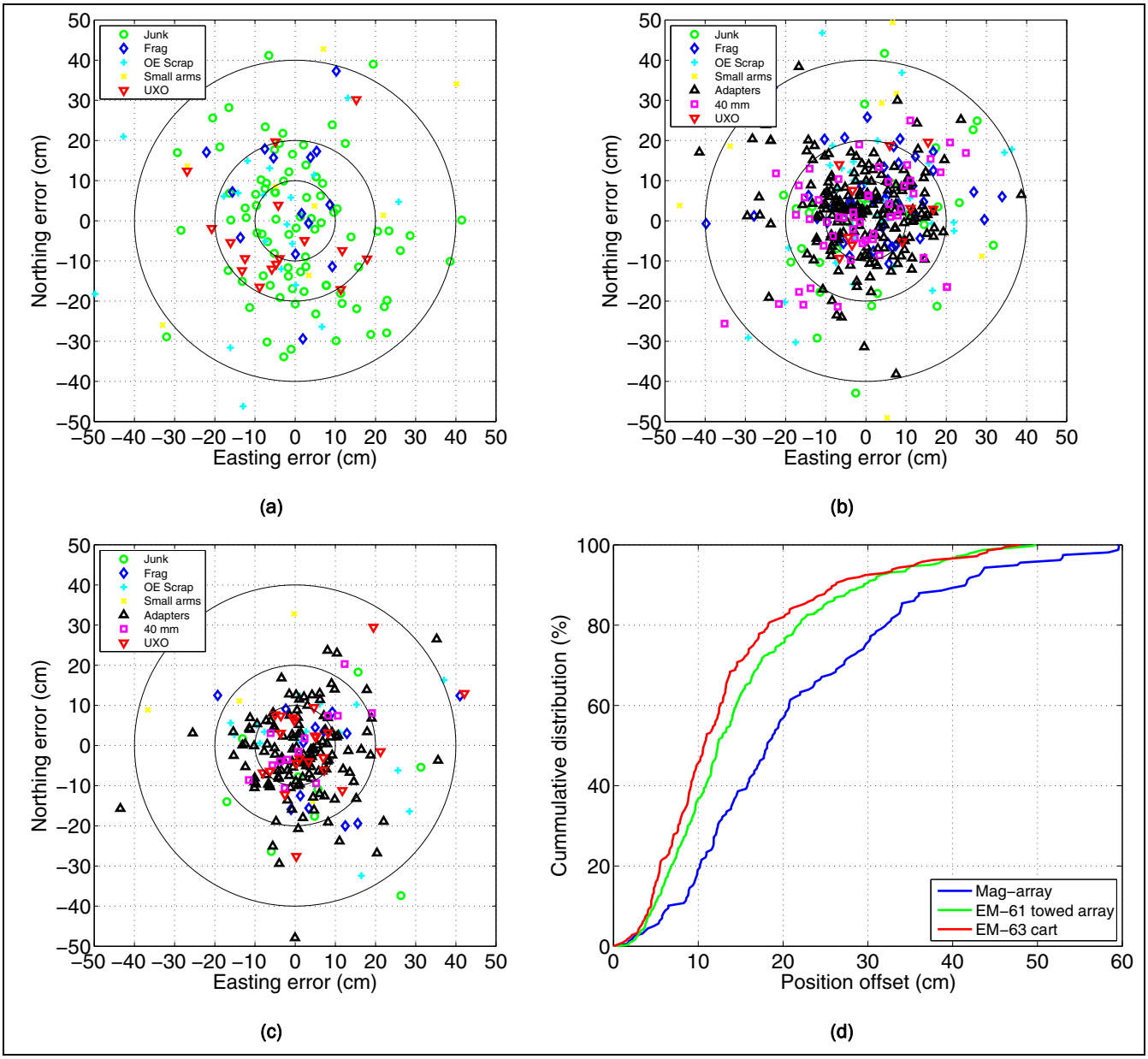

Figure 14. Comparison of predicted versus actual locations for dipole model fits to (a) magnetometer; (b) EM-61 towed-array; and (c) EM-63 cart data. Circles of radii 10, 20, and 40 cm are marked on each plot. A cumulative distribution of the position errors for each sensor is shown in (d).

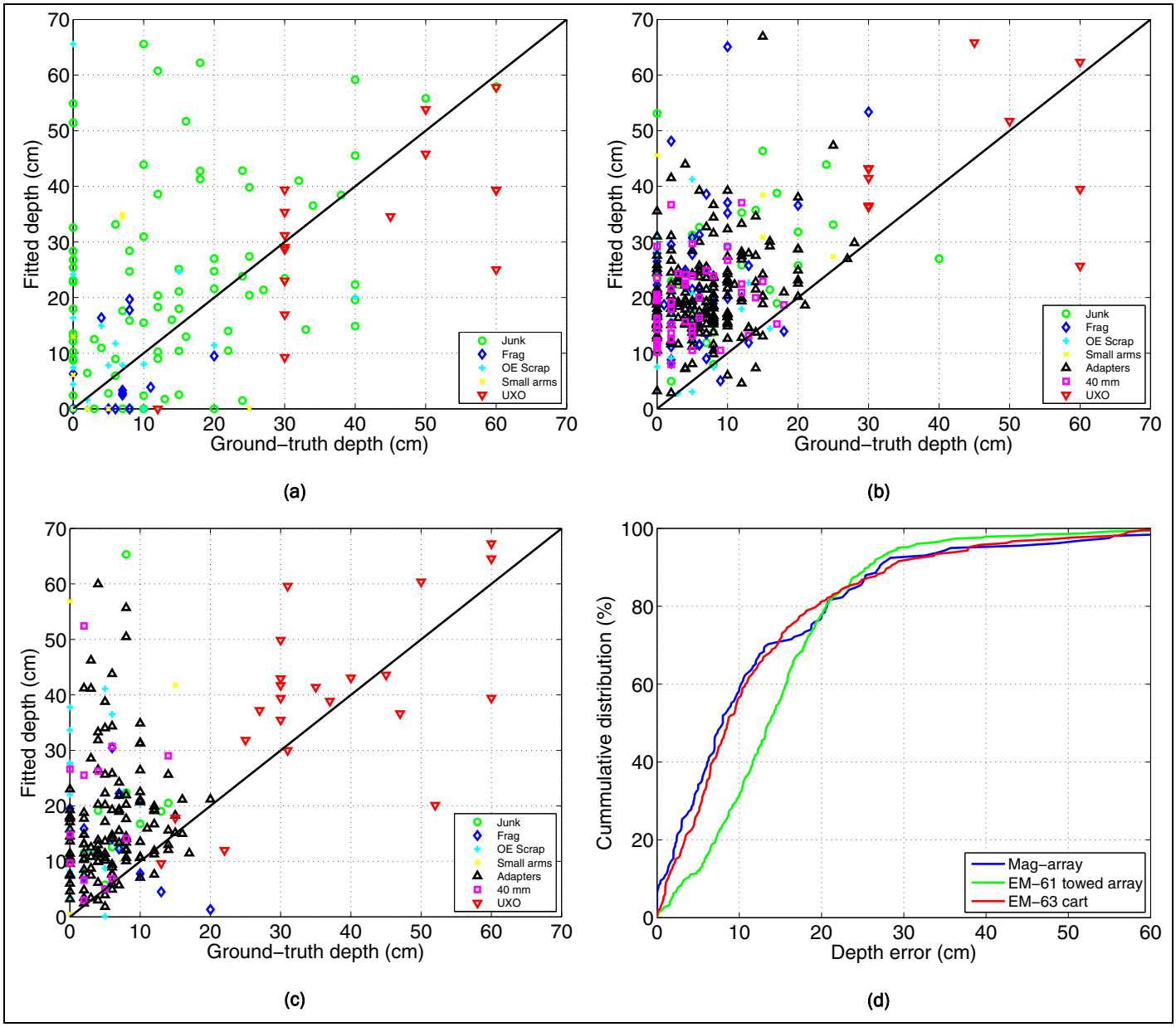

Figure 15. Comparison of predicted versus actual depths for dipole model fits to (a) magnetometer; (b) EM-61 towed-array; and (c) EM-63 cart data. A cumulative distribution of the error in depth recovery is shown in (d).

4 Statistical Classification of EM-61 and EM-63 Data

The qualitative observations on discrimination performance described in the previous section will now be quantified. The methodology described in Beran and Oldenburg (in preparation) was used to achieve this goal. As described in Report 6 of this series, once feature vectors have been obtained through inversion, the next step in the discrimination process is to train and apply a statistical classification algorithm. The remainder of this report uses a Probabilistic Neural Network (PNN) classifier, as initial experimentation indicated it would produce the best discrimination performance.

The performance of a discrimination strategy is often displayed using the ROC curve, which shows the true positive fraction (TPF) as a function of the false positive fraction (FPF). Here, the TPF is the proportion of UXOs found and the FPF is the proportion of clutter found. The ordinate is sometimes also displayed as the number of false alarms per acre, or simply the total number of clutter items dug. To generate an ROC curve for a discrimination algorithm, threshold on the output of that algorithm. As the threshold varies, the decision boundary sweeps through the feature space and increasing numbers of UXO and clutter are flagged for digging.

A metric of classifier performance that is derived from the ROC is the area under the curve (AUC). The AUC is defined as the integral of the true positive fraction with respect to the false positive fraction:

$$AUC = \int_0^1 TPF \; d(FPF) \tag{2}$$

If the FPF is the fraction of all test clutter items which are dug, then an ideal discrimination algorithm will have an AUC = 1 (i.e., all UXOs are found before a single clutter item is dug). Conversely, the worst possible classifier will require digging all clutter items before finding any UXO, producing an AUC = 0.

An alternative metric for measuring discrimination performance is the False Alarm Rate (FAR), defined as the proportion of clutter that must be

dug in order to find all UXOs. The FAR is defined graphically by the point at which the TPF first attains a value of one. Intuitively, the FAR can be regarded as an estimate of the probability that a randomly drawn scrap item is ranked ahead of the worst case (i.e., the minimum) prediction for all feature vectors belonging to the UXO class.

Any potential application of the performance metrics discussed above requires their estimation, ideally with an independent test data set. Generating such a test set may be possible when all anomalies in selected areas are cleared in an initial digging stage. In this case, performance can be estimated using previously trained classifiers on the newly labeled test feature vectors. However, at Camp Lejeune, excavations were nor formally structured into test and training datasets. At this point an arbitrary division of labeled data into training and test sets is undesirable: since there is potential to learn from all feature vectors, all labeled data are included in the training set. However, estimating performance is problematic if there are no independent test data. An algorithm that perfectly discriminates the training data may not generalize well to an unseen test set. This is analogous to over-fitting the data in regression, where fitting a noisy function too closely can produce poor estimates of the function parameters.

Cross-validation is a standard way to estimate discrimination performance when no independent test data are available. In “leave-one-out” cross-validation, a single vector is left out of the training set and the algorithm is trained on the remaining vectors. Discrimination can then be predicted for the hold-out vector and the process is repeated for all training vectors. The AUC or FAR can then be estimated from the set of cross-validation predictions. The training samples in this approach are substantially the same, and so if the classifier over-fits this training set, an overly optimistic estimate of discrimination performance will result (Beran and Oldenburg, in preparation).

This difficulty can be addressed with bootstrap estimation. If the full set of labeled data L comprises N feature vectors, the true (unknown) class distributions can be approximated as discrete distributions with all labeled vectors in L attributed equal weight $1/N$. Any desired statistic can be estimated by drawing samples from these empirical distributions. In practice, bootstrapping generates a training realization by sampling with replacement N times from L. This procedure will generate repeated feature

vectors in the training realization, so that the expected number of unique feature vectors is then:

$$\mathrm{E}\left[N_{bootstrap}\right] = \left[1 - (1 - 1/\mathrm{N})^{\mathrm{N}}\right]\mathrm{N} \approx 0.632\mathrm{N} \quad (3)$$

The remaining feature vectors (on average 1 - 0.632 = 0.368 of the vectors in L) can then be used as a hold-out test set to estimate the performance metrics. In discrimination problems, the "0.632" bootstrap estimator is the preferred estimator of discrimination performance statistics (Beran and Oldenburg, in preparation). This estimate is computed by:

1. Generating a bootstrap realization of training and test sets by sampling with replacement from the full set of labeled data.
2. Training the discrimination algorithm on the bootstrap training set.
3. Generating predictions for both the bootstrap training and test sets.
4. Estimating the performance statistic φ (e.g., FAR, AUC) of interest, again for both bootstrap training and test sets. For a given bootstrap realization B, this produces the estimates φ^{B}_{test} and φ^{B}_{train}.
5. Averaging the bootstrap performance statistics according to:

$$\varphi_{0.632} = 0.632\varphi^{B}_{test} + 0.368\varphi^{B}_{train} \quad (4)$$

6. Repeating steps 1–5 to obtain a distribution for $\varphi_{0.632}$.

4.1. Statistical classification using the EM-61

Figure 11 and the discussion in Section 3.2 indicated that a combination of magnitudes and ratio of instantaneous polarizations augmented by the magnetic field energy may achieve the stated discrimination objectives. Some initial experimentation narrowed the list of features down to $L_2(t_1)$, $L_2(t_4)/L_2(t_1)$, and magnetic energy. It was decided to train on classifier using $L_2(t_1)$ and $L_2(t_4)/L_2(t_1)$, and the other with $L_2(t_1)$ and magnetic energy to determine the impact on discrimination of the ancillary information provided by the magnetometer. The performance of dig-sheets is also ranked by magnetometer amplitude and by $L_2(t_1)$.

Figure 16 compares best, worst, and mean ROC curves computed through bootstrapping using 100 realizations, where the objective was to discriminate UXO and 40-mm grenades from adapters and other non-hazardous items. None of the four methods was particularly effective. The AUC_{62} and FAR_{62} measures (Table 2) are best for the PNN trained on $L_2(t_1)$ and $L_2(t_4)/L_2(t_1)$.

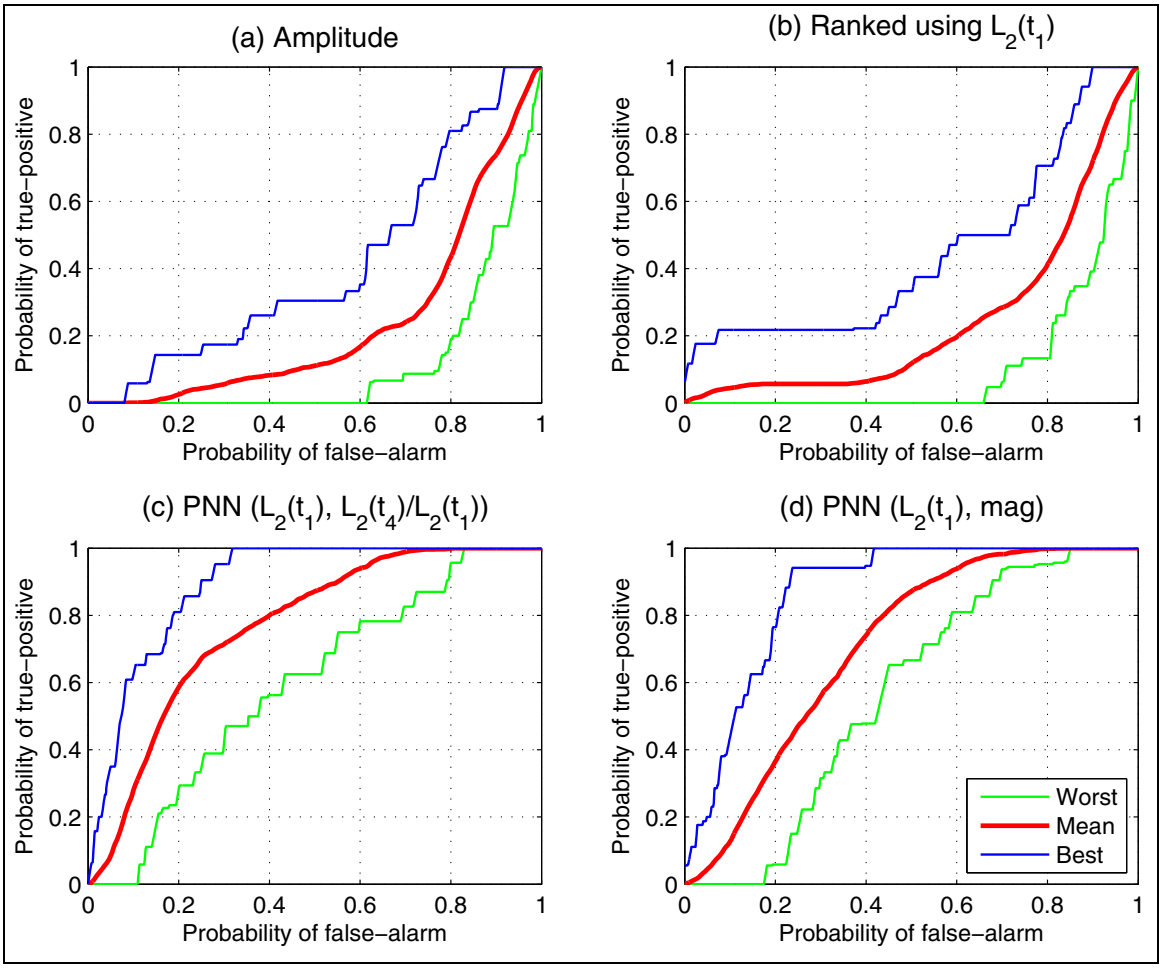

Figure 16. Comparison of best, worst, and mean ROC curves through bootstrapping of various discrimination methods applied to the EM-61 array data with an objective to distinguish UXO and 40-mm grenades from adapters: (a) ranking according to anomaly amplitude; (b) ranking on the basis of $L_2(t_1)$ (dig from largest to smallest); (c) PNN trained on $L_2(t_1)$ and $L_2(t_4)/L_2(t_1)$; and (d) PNN trained on $L_2(t_1)$ and magnetic-field energy.

Table 2. Comparison of statistical classifiers applied to the EM-61 towed-array data.

Method	Finding 40-mm grenades		Finding UXO	
	AUC	FAR	AUC	FAR
Amplitude	0.82	0.89	0.55	0.75
Size	0.75	0.71	0.87	0.32
PNN on $L_2(t_1)$, $L_2(t_4)/L_2(t_1)$	0.85	0.66	0.91	0.20
PNN on $L_2(t_1)$, magnetics	0.86	0.86	0.94	0.13

Simplifying the discrimination challenge by not including the 40-mm grenades, the performance of all methods is improved (Figure 17 and Table 2). The PNN trained on $L_2(t_1)$ has the best performance with AUC_{62} = 0.94 and FAR_{62} = 0.13. The PNN trained on $L_2(t_1)$ and $L_2(t_4)/L_2(t_1)$ is less effective on average and also shows a much larger variability in the results. The ratio of polarizations provides valuable information as the PNN is more effective than a ranking based on size alone. This result indicates that, when trying to reduce the number of excavated adapters, magnetic energy significantly improves the discrimination performance of the EM-61 cart and is more informative than the time-decay information.

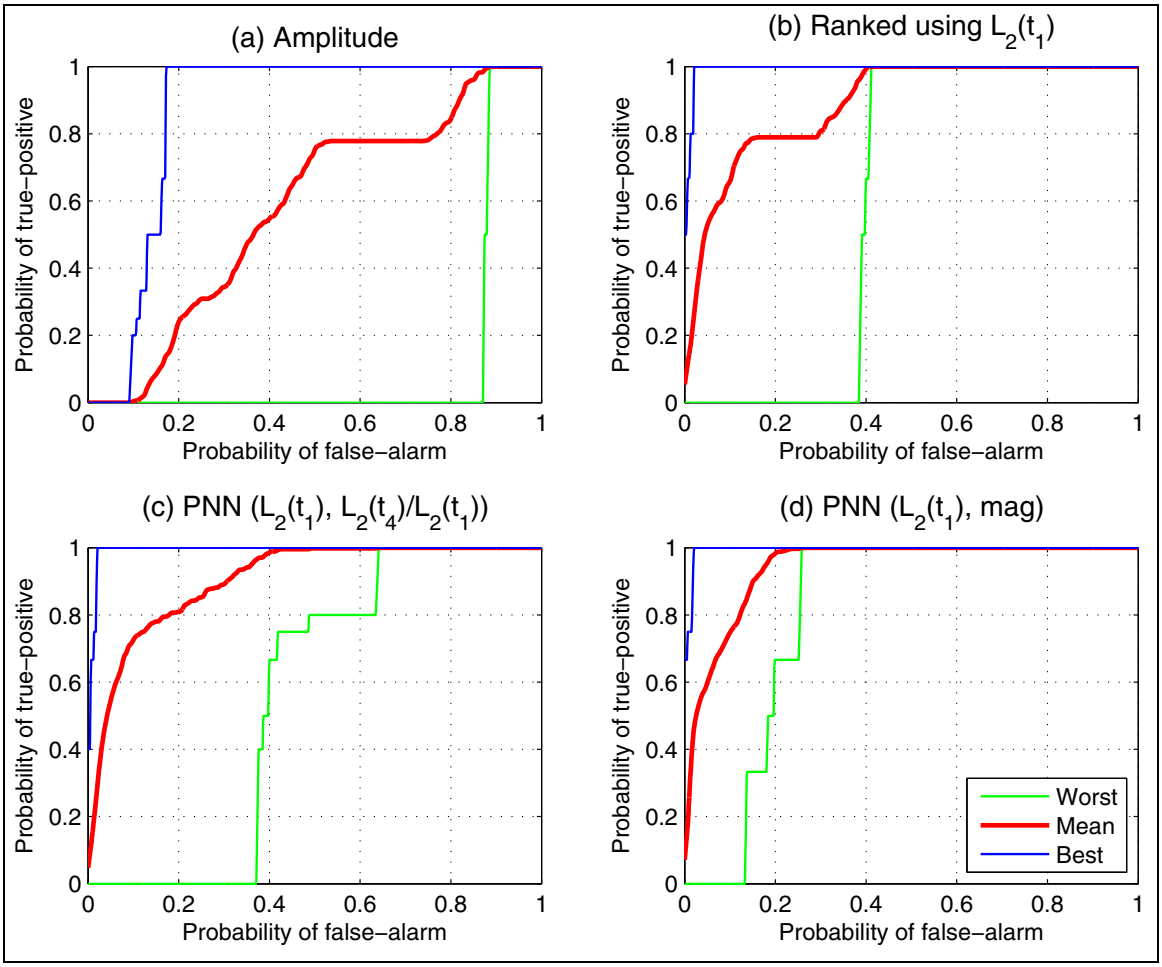

Figure 17. Comparison of best, worst, and mean ROC curves through bootstrapping of various discrimination methods applied to the EM-61 array data with an objective to distinguish UXO from adapters: (a) ranking according to anomaly amplitude; (b) ranking on the basis of $L_2(t_1)$ (dig from largest to smallest); (c) PNN trained on $L_2(t_1)$ and $L_2(t_4)/L_2(t_1)$; and (d) PNN trained on $L_2(t_1)$ and magnetic-field energy.

4.2. Statistical classification using the EM-63

Figures 12 and 13 and the associated discussion in Section 3.3 indicated that β_2, γ_2, and k_1 and/or k_2 might provide good discrimination performance against UXO, 40-mm grenades and adapters. Figure 18 compares best, worst, and mean ROC curves computed through bootstrapping using 100 realizations, where the objective was to discriminate UXO and 40-mm grenades from adapters and other non-hazardous items. Ranking according to amplitude gives the worst performance (Table 3) with AUC_{62} = 0.3 and FAR_{62} = 0.99. Determining the digging order using β_2 or using a PNN trained on k_1 and magnetic energy improves performance over amplitude. However, neither is as efficient as a PNN trained on k_1, β_2, and γ_2, which has the best performance with AUC_{62} = 0.79 and FAR_{62} = 0.4.

Simplifying the discrimination challenge by not including the 40-mm grenades improves the performance of all methods (Figure 19 and Table 3). The PNN trained on k_1, β_2, and γ_2 again has the best performance, with AUC_{62} = 0.94 and FAR_{62} = 0.13. Note that this result indicates that, when trying to reduce the number of excavated adapters, the time information recovered by the EM-63 is a more powerful discrimination diagnostic than the magnetic field energy.

Table 3. Comparison of AUC and FAR measures through bootstrapping of various discrimination methods applied to the EM-63 cart data.

Method	UXO and 40-mm grenades		UXO only	
	AUC	FAR	AUC	FAR
Anomaly amplitude	0.3	0.99	0.54	0.9
Size	0.77	0.66	0.85	0.29
PNN using k_1, β_2, γ_2	0.79	0.4	0.94	0.13
PNN using k_1, mag	0.71	0.88	0.89	0.25

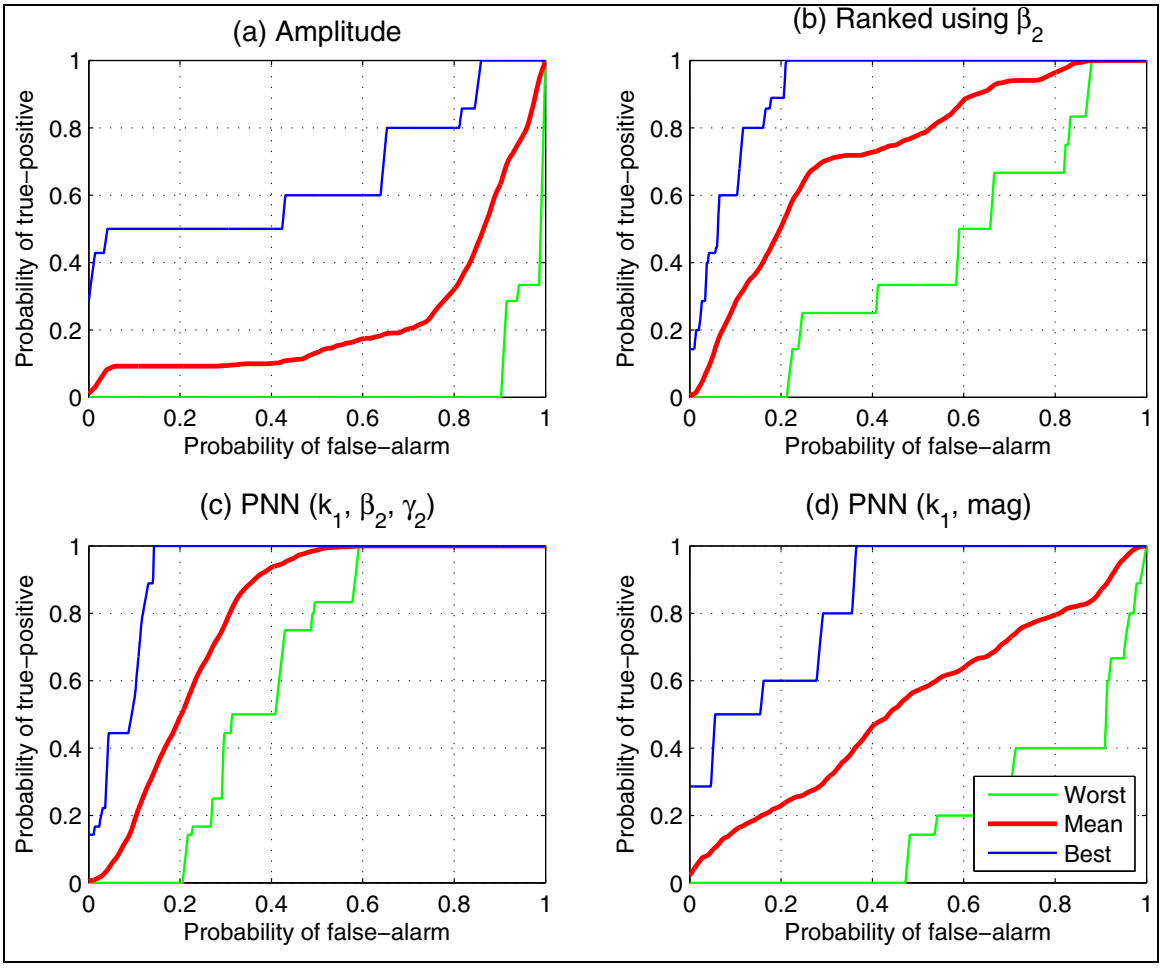

Figure 18. Comparison of best, worst, and mean ROC curves through bootstrapping of various discrimination methods applied to the EM-63 cart data with an objective to distinguish UXO and 40-mm grenades from adapters: (a) ranking according to anomaly amplitude; (b) ranking on the basis of β_1 (dig from largest to smallest); (c) PNN trained on k_1, β_2 and γ_2; and (d) PNN trained on k_1 and magnetic-field energy.

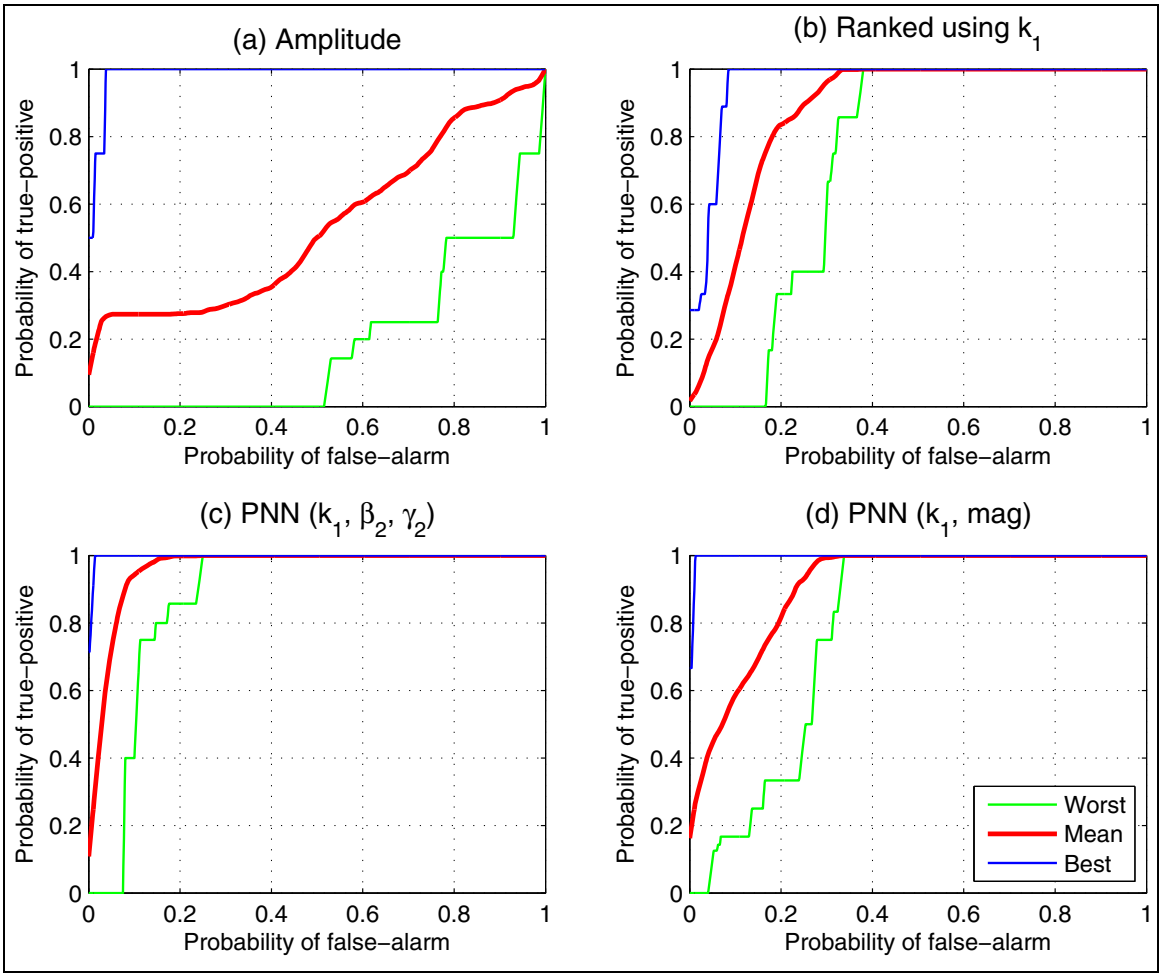

Figure 19. Comparison of best, worst, and mean ROC curves through bootstrapping of various discrimination methods applied to the EM-63 cart data with an objective to distinguish UXO from adapters: (a) ranking according to anomaly amplitude; (b) ranking on the basis of k_1 (dig from largest to smallest); (c) PNN trained on k_1, β_2, and γ_2; and (d) PNN trained on k_1 and magnetic-field energy.

5 Discussion

Camp Lejeune was the primary site used in this project for the evaluation of UXO detection and discrimination potential of GPR (see Report 7). In addition to the GPR data, three different types of geophysical data were collected: a man-portable magnetics array, an EM-61 towed array, and an EM-63 cart. Apart from 30 emplaced items, only one UXO of significant size was encountered on the site (a 120-mm HEAT rocket). The other potentially dangerous item found was a 40-mm smoke grenade, although most of them were inert practice rounds. Pervasive on the site were non-ferrous adapters, which comprised almost 40 percent of the items excavated. The discrimination challenge at the site was to identify larger ferrous UXO and the smaller 40-mm grenades, while preventing excessive excavations of adapters.

The insensitivity of magnetometry to non-ferrous metals makes it an ideal technique for rejecting false alarms due to the ubiquitous adapters present on the site. However, this same argument precludes using the technique for detection of the 40-mm grenades. For the UXO items, prioritizing digging order on the magnetic remanence metric is very effective when items don't exhibit large remanent magnetizations. A more conservative and safer method is to dig according to the size of the moment.

For the EM-61 towed array, the spread of secondary to tertiary polarizations, or the ratio of primary to secondary polarization of the three-dipole models did not provide any useful discrimination information. After turning the three-dipole models into equivalent two-dipole models, the size of $L'_2(t_1)$ allowed many adapters to be rejected. The relative decay rate of the primary or secondary polarizations can be used to distinguish many of the remaining adapters from the UXO. The standard deviation in a 0.5-m radius of the corresponding magnetic data was highly discriminatory against the adapters.

For the EM-63 cart data, the decay of the secondary polarization of the adapters was significantly different than that of the UXO. Consequently, the k, β, and γ feature vectors were very effective at discriminating UXO from adapters, and the 40-mm grenades from the adapters. This empirical observation was confirmed by conducting a bootstrap analysis on a PNN

trained on k_1, β_2, and γ_2. The results indicated that the longer measurement time of the EM-63 resulted in discrimination performance superior to the EM-61 and obviated the need for any supplemental magnetic data. For the UXO/adapter discrimination problem, the EM-61/magnetometer combination had comparable performance to the EM-63 alone. When the 40-mm grenades were included as potential UXO, the EM-63 significantly outperformed the EM-61/magnetometer combination.

References

Beran, L., and D. W. Oldenburg. Selecting a discrimination algorithm for unexploded ordnance remediation. In preparation, *IEEE Transactions Geoscience & Remote Sensing*.

Billings, S. D. 2004. Discrimination and classification of buried unexploded ordnance using magnetometry. *IEEE Transactions of Geoscience and Remote Sensing* 42:1241–1251.

Billings, S. D., L. R. Pasion, L. Beran, D. W. Oldenburg, D. Sinex, L. Song, and N. Lhomme. 2007. Demonstration Report for the Former Lowry Bombing and Gunnery Range, ESTCP MM-0504: Practical discrimination strategies for application to live sites.

Billings, S. D., L. R. Pasion, S. Walker, and L. Berans. 2006. Magnetic models of unexploded ordnance. *IEEE Transactions Geoscience & Remote Sensing*. 44:2115–2124.

Pasion, L. P., and D. W. Oldenburg. 2001. A discrimination algorithm for UXO using time domain electromagnetics. *Journal of Engineering and Environmental Geophysics* 28:91–102.

Appendix A: Diary of Site Activities

Table A1. List of daily activities at Camp Lejeune.

Day	Activity
	Pre-survey
Aug-05	Reconnaissance visit to site to determine suitability of site for GPR measurements and to view potential survey sites
Sept-05	Site characterization surveys performed by ERDC/Sky personnel
21-22-Feb-06	Emplacement of known ordnance at survey site for calibration over known targets
	Magnetometer
21-Feb-06	Arrive at site, unpack equipment, start mag surveys in southern tiles of G6 range (covered four 50-m x 50-m grids)
22-Feb-06	Complete survey of G6 range (covered eight 50-m x 50-m grids)
4-Mar-06	Survey of G5 range (two 50-m x 50-m sites)
5-Mar-06	Pack up equipment for deployment to different site
	EM-61 Towed Array
23-Feb-06	Arrive on site, set up towed array, and troubleshoot IMU issues
24-Feb-06	Started surveying on G6 range, collection ends early when sled breaks
25-Feb-06	Continue surveying on G6 range
26-Feb-06	Continue surveying on G6 range
27-Feb-06	Continue surveying on G6 range
2-Mar-06	G5 Range surveyed (100 m x 50 m), wrong RTS configuration, needs recollect, sled breaks
3-Mar-06	Repair and assemble towed array, survey G5 range. Problem with sensor 1, needs recollect
4-Mar-06	Reacquire G5 range data with all equipment functioning correctly
5-Mar-06	Pack up equipment for deployment to different site
	EM-63
24-Feb-06	Assemble EM-63 on new suspension cart and collected calibration measurements
25-Feb-06	Surveyed half of 50-m x 50-m grid A1 on G6 range
26-Feb-06	Completed coverage of grid A1 on G6 range
27-Feb-06	Suspension cart fails, downtime waiting for replacement parts and repairs
28-Feb-06	Survey 50-m x 50-m grid A2 on G6 range
1-Mar-06	Survey 50-m x 50-m grid E2 on G6 range, short day due to firing scheduled on adjacent range
2-Mar-06	Survey 50-m x 50-m grid E1 on G6 range
3-Mar-06	Survey two 50-m x 50-m grids (D1, D2) on G6 range
6-Mar-06	Start survey on two 50-m x 50-m grids on G5 range
7-Mar-06	Complete survey of two 50-m x 50-m grids on G5 range, cued interrogation of four G5 range targets
8-Mar-06	Cued interrogation of 15 G5 range targets
9-Mar-06	Survey for clean background area of G6 range to be used for test stand cued interrogation surveys, surveyed five G6 range-emplaced items in the A2 grid
10-Mar-06	Cued-interrogation over five emplaced items of G6 Range on the A1/A2 grids

Day	Activity
14-Mar-06	RTS troubleshooting, technicians indicated problem was an internal fiber-optic connection and unit would need to be returned for repair. In the interim, loaner system would be sent
15-Mar-06	Loaner RTS arrives without radio transmitter, cannot survey without it
16-Mar-06	Loaner radio transmitter arrives midday, surveying resumes in test stand configuration. At end of day, tablet PC dies and is unbootable
17-Mar-06	Dropped off dead tablet PC at computer store for repair attempts. Tried to install DAS on laptop to acquire data; however, additional drivers required to recognize multiple ports
20-Mar-06	New RTS unit arrives and necessary files to run DAS from laptop arrive. Tablet PC in parts at computer store, replacement on the way. Tested in hotel parking lot, system working with laptop
21-Mar-06	Cued-interrogation survey of six items in test stand configuration on the G6 range
22-Mar-06	Cued-interrogation survey of six items in test stand configuration on the G6 range. Start discrimination mode survey over G6 range grid D2
23-Mar-06	Complete discrimination mode survey of G6 range grid D2
24-Mar-06	Pack up equipment and ship
Validation	
28-Feb-06	Validation of 20 anomalies at G6 range (grids H1, H2) picked from magnetic data
6-Mar-06	Validation of 32 anomalies at G6 range (grids B1, B2)
7-Mar-06	Validation of 56 anomalies at G6 range (grids B1, B2)
8-Mar-06	Validation of 68 anomalies at G6 range (grids B1, B2)
9-Mar-06	Validation of 73 anomalies at G6 range (grids B1, B2)
10-Mar-06	Surface sweep records positions and removes 38 items on G6 range
13-Mar-06	Removed all emplaced items in G5 range due to active clearance work, transferred items to G6 range, D2 grid
15-Mar-06	Validation of 37 anomalies at G6 range (grids B1, B2)
17-Mar-06	Validation of 26 anomalies at G6 range (grids H1, H2)
18-Mar-06	Validation of 34 anomalies at G5 range
19-Mar-06	Validation of 32 anomalies at G5 range
20-Mar-06	Validation of 52 anomalies at G6 range, completing the H1, H2 grids
21-Mar-06	Validation of 32 anomalies at G6 range, G1 grid
22-Mar-06	Validation of 70 anomalies at G6 range, G1, A1 grids
23-Mar-06	Validation of 97 anomalies at G6 range, A1, A2 grids
25-Mar-06	Validation of 36 anomalies at G6 range, A2 grid. Removed emplaced items in A1, A2, D2 grids
26-Mar-06	Validation of 63 anomalies at G6 range, D1 grid
27-Mar-06	Validation of 92 anomalies at G6 range, D2, G2 grids
28-Mar-06	Validation of 149 anomalies at G6 range, E1, E2 grids

Appendix B: Items Emplaced on Site

Table B1. Items emplaced on the G6 range at Camp Lejeune (large ferrous ordnance only).

Item	Grid	ID	Easting(m)	Northing (m)	Depth (cm)	Dip (degs)	Azimuth (degs)	Sensors
105-mm Projectile – Inert	A1	1	294357.25	3833291.35	45	0	6	All
105-mm Projectile – Heat	A1	2	294354.91	3833301.11	50	45	94	All
81-mm mortar	A1	3	294353.00	3833310.05	30	90	n/a	All
2.75 in. Warhead Rocket	A1	4	294350.01	3833319.96	30	0	240	All
76-mm projectile (blue)	A1	5	294348.07	3833329.96	30	45	320	All
4.2-in. projectile (blue)	A1	6	294367.06	3833293.03	50	90	n/a	All
90-mm projectile (blue AP)	A1	7	294364.03	3833302.94	30	90	n/a	All
90-mm projectile (blue AP)	A1	8	294361.82	3833311.87	60	45	120	All
81-mm mortar (blue)	A1	9	294359.35	3833321.79	30	90	n/a	All
81-mm mortar (blue)	A1	10	294356.68	3833332.27	60	45	120	All
90-mm projectile (blue AP)	A2	11	294397.97	3833338.04	30	0	180	All
90-mm projectile (blue AP)	A2	12	294417.79	3833314.13	30	90	n/a	All
90-mm projectile (blue AP)	A2	13	294423.69	3833315.23	60	45	235	All
81-mm mortar (blue)	A2	14	294424.99	3833337.60	30	0	95	All
81-mm mortar (blue)	A2	15	294431.62	3833326.89	30	90	n/a	All
81-mm mortar (blue)	A2	16	294425.59	3833345.85	60	0	70	All
81-mm mortar (blue)	A2	17	294398.57	3833325.17	60	45	270	All
90-mm projectile	D2	18	294465.10	3833202.41	40	25	190	EM-63
3-in. rocket	D2	19	294466.32	3833197.91	25	30	20	EM-63
81-mm mortar	D2	20	294468.25	3833193.99	27	65	50	EM-63
3.5-in. rocket	D2	21	294469.35	3833189.11	35	5	220	EM-63
3.5-in. rocket	D2	22	294471.31	3833183.30	32	42	10	EM-63
105-mm projectile	D2	23	294472.72	3833176.11	22	2	30	EM-63
105-mm projectile	D2	24	294473.21	3833169.03	31	40	280	EM-63
3.5-in. rocket	D2	25	294469.39	3833160.16	15	40	20	EM-63
105-mm projectile	D2	26	294464.78	3833179.97	31	80	30	EM-63
3.5-in. rocket	D2	27	294461.79	3833188.40	13	39	150	EM-63
105-mm projectile	D2	28	294457.23	3833198.07	37	10	310	EM-63
3.5-in. rocket	D2	29	294461.95	3833197.71	52	90	360	EM-63
105-mm projectile	D2	30	294465.51	3833184.63	47	50	80	EM-63

REPORT DOCUMENTATION PAGE

Form Approved
OMB No. 0704-0188

1. REPORT DATE *(DD-MM-YYYY)*	2. REPORT TYPE	3. DATES COVERED *(From - To)*
September 2008	Report 8 of 9	

4. TITLE AND SUBTITLE

UXO Characterization: Comparing Cued Surveying to Standard Detection and Discrimination Approaches: Report 8 of 9 – Marine Corps Base Camp Lejeune: UXO Characterization Using Magnetic and Electromagnetic Data

5a. CONTRACT NUMBER
W912HZ-04-C-0039

5b. GRANT NUMBER

5c. PROGRAM ELEMENT NUMBER

6. AUTHOR(S)

Steven D. Billings, Leonard R. Pasion, Laurens Beran, Kevin Kingdon, and Jon Jacobson

5d. PROJECT NUMBER

5e. TASK NUMBER

5f. WORK UNIT NUMBER

7. PERFORMING ORGANIZATION NAME(S) AND ADDRESS(ES)

Sky Research, Inc.
445 Dead Indian Memorial Road
Ashland, OR 97520-9706

8. PERFORMING ORGANIZATION REPORT NUMBER

ERDC/EL TR-08-39

9. SPONSORING / MONITORING AGENCY NAME(S) AND ADDRESS(ES)

Headquarters, U.S. Army Corps of Engineers
Washington, DC 20314-1000
U.S. Army Engineer Research and Development Center
Environmental Laboratory
3909 Halls Ferry Road, Vicksburg, MS 39180-6199

10. SPONSOR/MONITOR'S ACRONYM(S)

11. SPONSOR/MONITOR'S REPORT NUMBER(S)

12. DISTRIBUTION / AVAILABILITY STATEMENT

Approved for public release; distribution is unlimited.

13. SUPPLEMENTARY NOTES

14. ABSTRACT

The collection, processing, interpretation, and analysis of electromagnetic (EM) and magnetometer data collected at Camp Lejeune are described. The discrimination challenge at the site was to identify larger ferrous UXO and the smaller 40-mm grenades while preventing excessive excavations of adapters. For EM-61 towed array data, the relative size of primary and secondary polarizations allowed many adapters to be rejected. The relative decay rate of the primary or secondary polarizations was effective in distinguishing many of the remaining adapters from the UXO. The standard deviation in a 0.5-m radius of the corresponding magnetic data was also highly discriminatory against the adapters. For the UXO/adapter discrimination problem, the EM-61/magnetometer combination had comparable performance to the EM-63 alone. When the 40-mm grenades were included as potential UXO, the EM-63 significantly outperformed the EM-61/magnetometer combination.

15. SUBJECT TERMS

EMI sensors
Frequency-domain electromagnetic induction (FEM)
Ground penetrating radar
Time-domain electromagnetic induction (TEM)
Total-field magnetics
Unexploded ordnance (UXO)
UXO discrimination

16. SECURITY CLASSIFICATION OF:			17. LIMITATION OF ABSTRACT	18. NUMBER OF PAGES	19a. NAME OF RESPONSIBLE PERSON
a. REPORT	b. ABSTRACT	c. THIS PAGE			19b. TELEPHONE NUMBER *(include area code)*
UNCLASSIFIED	UNCLASSIFIED	UNCLASSIFIED		50	